Evaluating Streamflow Forecasts in Hydro-Dominated Power Systems–When and Why They Matter

Rachel Koh[1] and Stefano Galelli[2]

[1]Singapore University of Technology and Design
[2]Cornell University

August 7, 2023

Abstract

The value of seasonal streamflow forecasts for the hydropower industry has long been assessed by considering metrics related to hydropower availability. However, this approach overlooks the role played by hydropower dams within the power grid, therefore providing a myopic view of how forecasts could improve the operations of large-scale power systems. With the aim of understanding how the value of streamflow forecasts penetrates through the power grid, we developed a coupled-water energy model that is subject to reservoir inflow forecasts with different levels of accuracy. We implement the modelling framework on a real-world case study based on the Cambodian grid, which relies on hydropower, coal, oil, and imports from neighboring countries. In particular, we evaluate the performance in terms of metrics selected from both the reservoir and power systems, including available and dispatched hydropower, power production costs, CO2 emissions, and transmission line congestion. Through this framework, we demonstrate that streamflow forecasts can positively impact the operations of hydro-dominated power systems, especially during the transition from wet to dry seasons. Moreover, we show that the value largely varies with the specific metric of performance at hand as well as the level of operational integration between water and power systems.

Evaluating Streamflow Forecasts in Hydro-Dominated Power Systems–When and Why They Matter

Rachel Koh [1], Stefano Galelli [1,2]

[1]Pillar of Engineering Systems and Design, Singapore University of Technology and Design, Singapore
[2]School of Civil and Environmental Engineering, Cornell University, Ithaca, NY

Key Points:

- The benefits of streamflow forecasts trickle down from the water to the power system
- Forecasts are particularly useful during the transition from wet to dry seasons
- The relationship between forecast skill-value is controlled by the level of operational integration between the two systems

Corresponding author: Rachel Koh, `kohzq.rachel@gmail.com`

Abstract

The value of seasonal streamflow forecasts for the hydropower industry has long been assessed by considering metrics related to hydropower availability. However, this approach overlooks the role played by hydropower dams within the power grid, therefore providing a myopic view of how forecasts could improve the operations of large-scale power systems. With the aim of understanding how the value of streamflow forecasts penetrates through the power grid, we developed a coupled-water energy model that is subject to reservoir inflow forecasts with different levels of accuracy. We implement the modelling framework on a real-world case study based on the Cambodian grid, which relies on hydropower, coal, oil, and imports from neighboring countries. In particular, we evaluate the performance in terms of metrics selected from both the reservoir and power systems, including available and dispatched hydropower, power production costs, CO_2 emissions, and transmission line congestion. Through this framework, we demonstrate that streamflow forecasts can positively impact the operations of hydro-dominated power systems, especially during the transition from wet to dry seasons. Moreover, we show that the value largely varies with the specific metric of performance at hand as well as the level of operational integration between water and power systems.

Plain Language Summary

Forecasts of river streamflow are regularly used by water system operators to plan the operations of large-scale infrastructures, such as hydropower dams. To date, research has focussed primarily on how the accuracy, or skill, of forecasts translates into added performance of reservoir systems, thereby overlooking the potential benefits for other interconnected infrastructures that depend on water availability. Here, we focus on the case on national power grids, whose performance is partially controlled by hydropower production. We show that the use of streamflow forecasts could bring benefits that 'trickle down' to power system operations, reducing, for instance, power production costs and CO_2 emissions during specific periods.

1 Introduction

Water managers often rely on streamflow forecasts to inform reservoir release decisions (Turner et al., 2020). As opposed to operating reservoir networks with static rule curves, streamflow forecasts offer operators the ability to dynamically adapt to anticipated inflow conditions (Troin et al., 2021). Accurate streamflow forecasts have been found to benefit multiple aspects of water management, such as flood control, water supply reliability, or hydropower production (Nayak et al., 2018; Delaney et al., 2020). The metrics used to assess the benefits, or value, of streamflow forecasts can be broadly classified under two categories. Under the first category, benefits are defined in terms of deviations from a pre-defined target, usually the target storage or release (Li et al., 2014; Turner et al., 2017). Under the second category, benefits are defined through metrics measuring the improvement in performance with respect to one or multiple objectives. Examples include reduction in water shortage (Nayak et al., 2018) or spilled water volume (Anghileri et al., 2016), better flood control (Wang et al., 2012; Galelli, Goedbloed, et al., 2014), and hydropower generation or revenue (Anghileri et al., 2019; Ahmad & Hossain, 2020; Doering et al., 2021; Guo et al., 2021; Lee et al., 2022). The common denominator among these metrics is that they are based on the output produced by a reservoir system model.

In hydro-dominated power systems, reservoir operations can have profound effects on power system operations (Voisin et al., 2020; Chowdhury et al., 2021; Chowdhury, Dang, et al., 2020). During dry conditions, for instance, a decrease in hydropower production may force power grid operators to raise production from thermoelectric plants, leading to higher operating costs and CO_2 emissions (Kern et al., 2020; Chowdhury et al., 2021). Defining streamflow forecast value solely in terms of water-related metrics thus overlooks the role played by hydropower reservoirs in the power grid. In this regard, it is worth stressing that there are only a handful of studies that evaluated whether the use of streamflow forecasts brings value to power grid operations (Ding et al., 2021; Gong et al., 2021). Both studies were conducted at the scale of a river basin—rather than on a spatial domain encompassing a national or regional grid—and adopted performance metrics defined in terms of power production only (i.e., supply from hydropower, wind, and solar photovoltaic). Hence, an in-depth understanding of how power system operations could benefit of streamflow forecasts is missing. In particular, it is important to understand which performance metrics are improved by the use of streamflow forecasts, when forecasts are most useful, and how forecast skill translates into different performance metrics. All these aspects would indeed be relevant to support the operationalization of streamflow forecasts.

Here, we aim to advance the current body of knowledge by studying how the value of streamflow forecasts unfolds as we move beyond a water reservoir system to include the operations of a national power grid. The questions of interest are therefore the following: How does forecast value change as we consider different performance aspects of a power grid? When is the use of forecasts more beneficial? How does forecast skill affect power system operations? Is forecast value affected by the interdependencies of the water-energy system? With the aid of a reservoir and power system model, we answer these questions by evaluating the value of streamflow forecasts for the operations of the Cambodian power system, which largely relies on the hydropower sector (Section 2 and 3). The criteria used in such evaluation are multiple metrics taken from both the reservoir and power systems, including available hydropower, dispatched hydropower (i.e., hydropower used within the grid), power production costs, CO_2 emission, and transmission line stress (Section 4). By simulating the coupled water-energy system with and without streamflow forecasts, we show that forecasts are particularly useful during the transition from the summer monsoon to the dry season. We also quantify the relationship between forecast skill and value, and show that forecast error is less important for production costs and CO_2 emissions, which are also impacted by electricity demand. We finally study how different levels of integration between water and power systems reshapes the skill-value relationship (Section 5).

2 Case study and Data

2.1 Case study

We carried out our analysis on the Cambodian water-energy system, illustrated in Figure 1. The representation of the system is based on the infrastructure built and operated in 2016, for which detailed data are available (Chowdhury, Kern, et al., 2020). Power supply is largely controlled by a network of six hydropower dams, which have a total installed capacity of 1,048 MW (see Table 1). In this reservoir network, there are two embankment dams (Kirirom I and Kirirom III), two dams operated in cascade (Atay and LR Chrum), and two headwater dams (Kamchay and Tatay). As we shall see, their production shows a pronounced inter-annual pattern; production increases during the summer monsoon (typically between May and October) and decreases during the dry season. The hydropower production is complemented by a few additional resources, namely thermoelectric plants (three coal-fired units totaling 400 MW of installed capacity and 15 oil-fired units totaling 282 MW), and import from neighboring countries (Thailand, Laos, and Cambodia). Taken together, all these resources are designed to meet the peak demand of 1,068 MW (EDC, 2016).

2.2 Data

Different datasets were obtained as inputs to the reservoir and power system models. Inputs to reservoir system model include reservoir specifications (Table 1) and time series of observed inflow and inflow forecasts. Since long and reliable time series of observed river discharge are not available, we retrieved inflow data for the six reservoirs from the

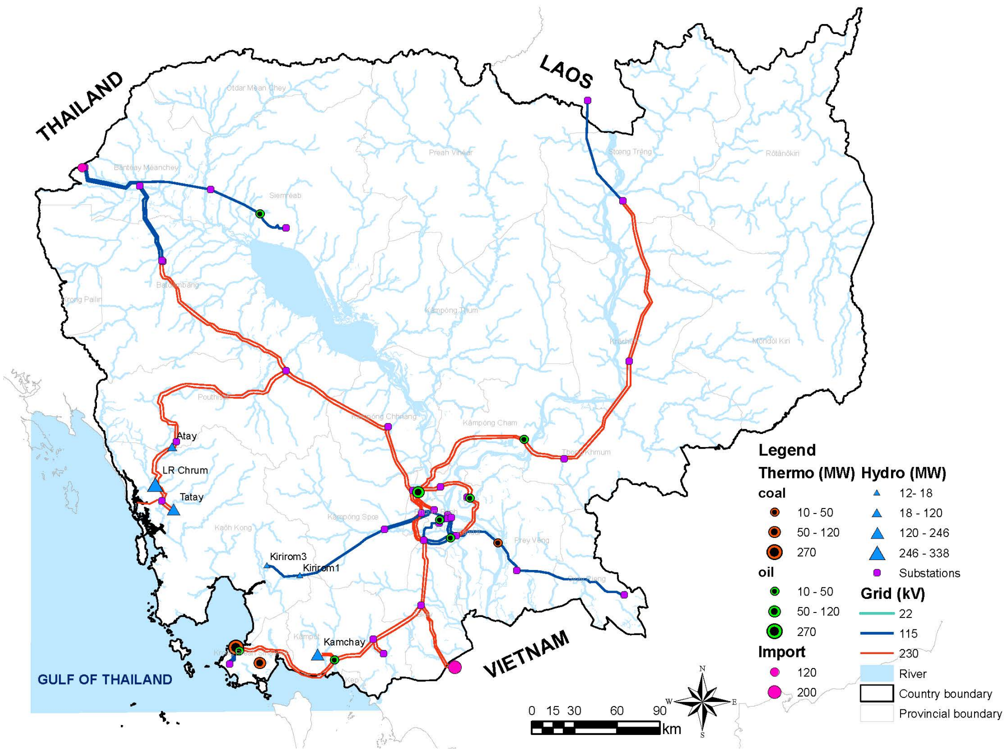

Figure 1. Main components of the Cambodian water-energy system, as of 2016. The circles represent the thermoelectric plants (coal and oil) and imports from neighbouring countries, while the triangles represent the hydropower plants. The purple squares and segments denote the substations and transmission lines, respectively. The river network is shown in light blue. Further details are provided in Section 2.1

.

Table 1. Design specifications of the Cambodian hydropower dams (EDC, 2016).

Name	Installed capacity (MW)	Dam height (m)	Storage (Mm^3)	Design discharge (m^3/s)	Hydraulic head (m)	Basin area (km^2)
Kamchay	194.1	110	680	163.5	122	710
Kirirom I	12	34	30	20	373.5	99
Kirirom III	18	40	30	40	271	105
Atay	240	45	443.8	125	216	1,157
LR Chrum	338	68	62	300	132	1,550
Tatay	246	77	322	150	188	1,073

Global Flood Awareness System (GloFAS) (Harrigan et al., 2021), a data source that (i) is commonly used in developing Asian countries (MacLeod et al., 2021) and (ii) allows us to model the water-energy system with a reasonable degree of accuracy (Koh et al., 2022). For consistency, we adopted the streamflow forecasts issued by GloFAS, which consists of an 11-member ensemble (Zsoter et al., 2020). The inflow data are available from 1979 to near real-time with daily resolution. Inflow forecasts are available for two days weekly (every Monday and Thursday) with a 24-hour time step and up to 46-day lead time. Forecasts are available from January 1999 to December 2018. The common period (2000-2018) was selected for all experiments.

For the power system model, required data include the specifications of the transmission lines and generators, as well as hourly time series of electricity demand at each substation. The line and generator details were extracted from technical reports (EDC, 2016; JICA, 2014), while the monthly peak demand was retrieved from the same reports. Based on the available monthly peak demand and hourly demand profiles for weekdays and weekends, we distribute the national demand to each substation on the basis of its voltage level. The detailed methodology for deriving the electricity demand time series is reported in Koh et al. (2022).

3 Modelling framework

3.1 Overview

As illustrated in Figure 2, the components of our computational framework are (1) a reservoir system model, (2) a power system model, and (3) a reservoir re-operation model. Note that the 'typical' representations of water-energy models include only the first two components: the reservoir model releases water according to its operating rules, and the amount of available hydropower is communicated to the power system model, which then dispatches (part of) the available hydropower depending on the specific dynamics of the power grid. This approach of separately modelling the water and power systems with a one-way information flow is known as 'soft-coupling' (Voisin et al., 2006; Chowdhury, Kern, et al., 2020; Kern et al., 2020). In our framework, we also use a reservoir re-operation model that explicitly accounts for the feedback from the power to the water system. In particular, the re-operation model gathers information on the amount of hydropower dispatched into the grid and calculates the corresponding amount of water that should be released from the dams (more details in Section 3.4). By engaging this component, the reservoir and power system models are 'hard-coupled', thus representing a situation in which the reservoir operations are contingent upon the state of the power system (Ibanez et al., 2014; Gebretsadik et al., 2016; Koh et al., 2022).

In our study, we evaluate the value of streamflow forecasts in the Cambodian grid by first operating the system with the soft-coupling approach. Doing so has two advantages. First, the unidirectional information flow provides insights into how the value of streamflow forecasts changes as we move from performance metrics focussing on the reservoir system to metrics focussing on the power system. Second, the lack of a tight operational integration between the two systems yields a larger operating space, allowing us to identify stressors (e.g., forecast skill) that control system performance—and that could be 'masked' by the presence of the feedback between the energy and water system. In the second part of our experiments, we incorporate the feedback mechanism between the systems by introducing the reservoir re-operation model. This adds one more stage to the modelling process, where the amount of hydropower dispatched by the power system is communicated back to the reservoir system model. Doing so provides insights into how the role played by streamflow forecasts within the power grid changes when the operating space is reduced.

3.2 Reservoir system model

The daily amount of hydropower available at each reservoir is determined by the reservoir system model through its release decisions, which can be determined by two alternative schemes: (i) a benchmark one based on static rule curves, and (ii) a more complex scheme that dynamically integrates the streamflow forecasts.

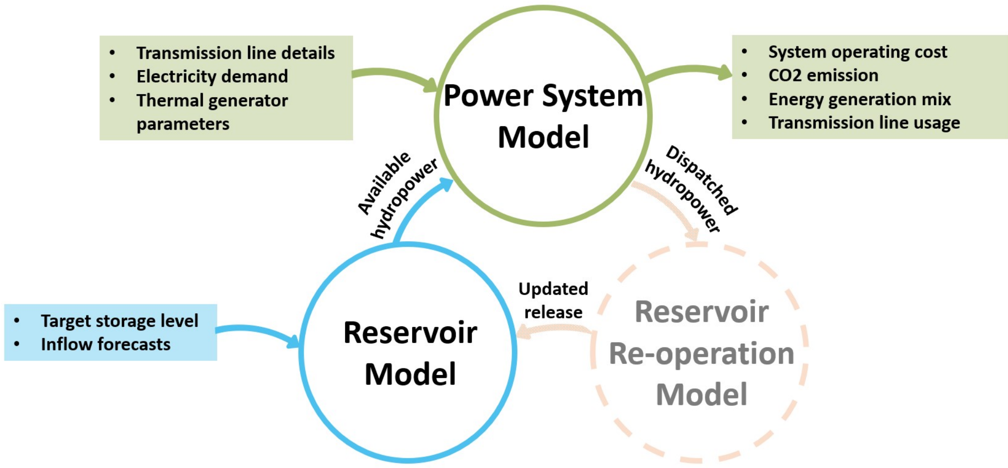

Figure 2. Schematic of the computational framework, comprising a reservoir system model, a power system model, and a reservoir re-operation model. The arrows represent the information flow between modelling components. The circles for the reservoir and power system models are in solid lines to represent the fact that these components are 'typically' considered in water-energy studies, where a water model provides the boundary conditions for a power system model. The dashed circle around the re-operation model indicates that this is an optional model that can be engaged when needed.

3.2.1 Benchmark scheme: rule curves

The storage dynamics of the i-th reservoir are described by the following mass balance, solved with a daily time step:

$$
\begin{aligned}
S_d^i = S_{d-1}^i + Q_d^i - R_d^i - spill_d^i - E_d^i,\\
0 \leq S_d^i \leq S_{cap}^i,\\
Q_{MEF,d}^i \leq R_d^i \leq R_{max}^i,
\end{aligned}
\tag{1}
$$

where S_d^i is the reservoir storage on day d, Q_d^i the reservoir inflow (between day $d-1$ and d), R_d^i the volume of water released through the turbines, $spill_d^i$ the volume of water spilled from the reservoir, E_d^i the evaporation losses from the dam, and S_{cap}^i the capacity of the dam.

An example of the rule curves we adopted is illustrated in Figure S1 (in the SI). Each rule curve is composed of a piecewise linear function based on the maximum and minimum water levels that the reservoir should reach within a calendar year (H_1^i and H_2^i) and the time of year in which these values should be reached (T_1^i and T_2^i). The concept of defining reservoir operating rule curves in this manner was proposed by Oliveira and Loucks (1997) and subsequently adapted in several other studies (e.g., Liu et al. (2011); Yassin et al. (2019)). Its use in representing actual system operations in Southeast Asia has also been validated (Chowdhury, Kern, et al., 2020; Dang et al., 2020). As an offline operating policy, the daily release decision R_d^i is made to bring the actual storage as close to the target storage as possible, while being subjected to an upper bound (R_{max}^i) and lower bound ($Q_{MEF,d}^i$). R_{max}^i is the maximum volume of water that can be turbined (representing the designed discharge capacity of the dam), while $Q_{MEF,d}^i$ represents the downstream environmental flow requirement, calculated according to the method used in Pastor et al. (2014).

Finally, the daily available hydropower for the i-th reservoir is calculated as follows:

$$HP_d^i = \eta \times \rho \times g \times R_d^i \times (H_{d-1}^i + H_d^i)/2, \tag{2}$$

where HP_d^i is the available hydropower (MW) on day d, η the turbine efficiency, ρ the water density (1000 kg/m^3), g the gravitational acceleration (9.81 m/s^2), and H_d^i the hydraulic head, taken as the average between days $d-1$ and d. For dams operated in cascade, Eq. (1) is updated to account for the natural inflow as well as the turbined and spilled water from the upper reservoir(s).

3.2.2 Forecast-informed scheme

In contrast to the benchmark scheme—where the reservoir release is only contingent upon the target water level—operating with streamflow forecasts allows the operators to make release decisions based on the knowledge available for the future inflows. In turn, this allows the system to prepare for impending wet or dry events. To integrate this information, the reservoir operation scheme employs a deterministic Model Predictive Control (MPC) approach (Galelli, Goedbloed, et al., 2014; Turner et al., 2017; Lee et al., 2022). According to this scheme, at the beginning of day d, the model receives a deterministic streamflow forecast for the next H days for each reservoir i ($Q_d^{f,i}, \ldots, Q_{d+H-1}^{f,i}$), and optimizes the release over that finite horizon (i.e., days $[d, d+H-1]$) according to a pre-defined objective function. In our work, consistent with the operating rules, we seek to explicitly maximize the hydropower generated by each dam. To prevent an over-aggressive release profile, we impose a penalty on the final state of the reservoir storage at the end of the forecast horizon (Soncini-Sessa et al., 2007), ensuring that it does not deviate too much from the target water levels (Figure S1). This yields the following optimization problem for each reservoir i:

$$\max_{R_d^i, R_{d+1}^i, \ldots, R_{d+H-1}^i} \sum_{t=d}^{d+H-1} HP_t^i - X(s_{t=d+H-1}^i), \tag{3}$$

where HP_t^i is the amount of hydropower produced by the i-th reservoir in one day and $X(\cdot)$ is the penalty associated to the storage on day $(d+H-1)$. HP_t^i is derived from Eq. (2) as a result of iteratively solving, over H days, Eq. (1) with Q_d^i replaced by the streamflow forecast $Q_d^{f,i}$. The release decisions are thus bounded by $Q_{MEF,d}^i$ and R_{max}^i. The output of the optimization problem (block of H days) is a time series of release decisions $R_d^i, R_{d+1}^i, \ldots, R_{d+H-1}^i$. Contingent upon the actual inflow (Q_d^i), we implement the release for the first day (R_d^i), and calculate the mass balance for each reservoir according to Eq. (1). The actual hydropower produced (HP_d^i) derived through Eq. (2) is then communicated to the power system model for dispatch. In sum, prior to each day d, we solve multiple MPC problems (one for each hydropower reservoir) with the aim of maximizing the hydropower generation for each reservoir over the next H days, yielding a sequence of reservoir releases as decision variables ($R_d^i, R_{d+1}^i, \ldots, R_{d+H-1}^i$).

3.3 Power system model

The power system model is PowNet, a production cost model that solves a mixed integer linear program with the objective of fulfilling the hourly electricity demand at minimum cost (Chowdhury, Kern, et al., 2020). The decisions made by PowNet include, for the next 24 hours, (i) which generating units to start-up and shut down (unit commitment) and (ii) the amount of power supplied by each unit (economic dispatch). Key inputs to PowNet include transmission line parameters, hourly time series of electricity demand at each sub-station, techno-economic parameters of thermoelectric generators (e.g., capacity, operations and maintenance costs), and the hydropower available at each dam calculated by the reservoir system model (Section 3.2). In scheduling the hourly production, the model is subject to multiple constraints, including ramping limits, generation limits, minimum up and down-time of each generator, and transmission capacity constraints. The decision variables at each hour thus include binary variables (e.g., generating unit to use and whether to switch it on or off) and continuous ones (e.g., electricity generated by each unit, voltage angle at each node, spinning and non-spinning reserves, amount of renewables and imports dispatched). For each simulated day, PowNet outputs include hourly time series of operating costs, CO_2 emissions, generation mix, and transmission line usage. PowNet has been applied to multiple national grids, such as the ones of Cambodia (Chowdhury, Kern, et al., 2020), Laos (Chowdhury, Dang, et al., 2020), and Thailand (Chowdhury et al., 2021; Galelli et al., 2022).

3.4 Reservoir re-operation model

The reservoir re-operation model is introduced as a means to capture the feedback between interdependent water-energy systems. Serving as a bridge between the reservoir and power system, this model compares the amount of available hydropower produced by the i-th reservoir (HP_d^i) with the amount dispatched by the power system (HP_d^{i*}). With the goal of reducing the mismatch between these two values, the re-operation is triggered when there is an over-production of hydropower (i.e., $HP_d^{i*} < HP_d^i$). The re-operation algorithm (refer to Koh et al. (2022) for details) then re-calculates the reservoir release such that the i-th reservoir releases only the amount R_d^{i*} ($< R_d^i$) needed to produce HP_d^{i*}. In this study, all reservoirs are re-operated in the scenario where the feedback between the systems is considered. Operating in this manner offers flexibility whereby the release decisions made by the hydropower reservoir can be updated based on real-time information regarding the power system. In other words, this allows each reservoir to be used as a 'battery', so water can be stored for future use. Doing so may alter the value of forecasts, as the operations of the reservoirs would then depend on the state of the power system as well.

4 Experimental setup

The goal of our study is to quantify the value of streamflow forecasts for power system operations, understand how the value changes with skill, and determine when the value matters the most. We use multiple benchmarks to characterize system operations under different conditions and thus meet our goals. First, we use the benchmark scheme (Section 3.2.1), i.e., static rule curves, to characterize reservoir operations. Subsequently, we compare the results to the forecast-informed scheme. Here, we introduce two benchmarks, perfect forecasts and climatology, both commonly used to assess the value of streamflow forecasts (Grantz et al., 2005; Zhao et al., 2012; Yossef et al., 2013; Zimmerman et al., 2016; Nayak et al., 2018; Anghileri et al., 2019; McInerney et al., 2020; Quedi & Fan, 2020). To characterize the skill-value relationships, we have at our disposal multiple forecasts within the ensemble, so one could perform weighted aggregation on the members or consider each member as a separate deterministic forecast (Slater et al., 2016; Delaney et al., 2020). We consider both, that is, (i) we take the ensemble mean across the 11 members (more details in Section 2.2), and (ii) we use the individual members as independent inputs. In sum, we run our simulations under 14 different forecast scenarios—i.e., perfect forecasts, climatology (taken as a 365-calendar day average from the inflow data), ensemble mean, and each of the 11 members. Taking into account how system operations may depend on the state of the power system as well, we repeat the experiments with the feedback from the power system back to the reservoir model. This means that our experiments are conducted (i) with 14 different deterministic forecast scenarios, and (ii) without and with feedback.

The forecast horizon selected in our study is 30 days based on the power generation mix obtained by preliminarily testing the system operations with different forecast horizons (see Table S1 in the SI for additional details). Since the reservoirs in our model are operated at the daily time step while the forecasts are only available on every Monday and Thursday of each week (Zsoter et al., 2020), we fill the gaps (Tuesday-Wednesday, Friday-Sunday) by extracting a 30-day window from the 46-day availability, and shifting the forecast one-day ahead, until the next set of forecasts is available. For example, the forecast for a given

Monday would be from day 1 to day 30 (out of the available 46 days), and the forecast for Tuesday would be from day 2 to 31 for the same set of 46 days. This is repeated for Wednesday; on Thursday, a new set of forecast is available again. Based on simulations ran on an Intel(R) Core (TM) i7-8700 CPU 3.2 GHz with 8 GB RAM running Windows 10, the runtime is approximately 20 hours for each simulation. The total runtime for 14 scenarios is thus approximately 280 hours. The experiments including the feedback from the power to the water system are more computationally demanding, taking about 40 hours each to complete.

Moving to the specific metrics that can be used to quantify forecast skill for deterministic forecasts, it is worth stressing that the options are many (Huang & Zhao, 2022). In this study, we considered the use of the Nash-Sutcliffe efficiency (NSE) (Nash & Sutcliffe, 1970), Pearson correlation coefficient (Lima & Lall, 2010; Li et al., 2014) and Symmetric Mean Absolute Percentage Error (SMAPE) (Ogliari et al., 2021). Since the forecast skill is calculated for each reservoir within the system, a spatial aggregation is necessary to represent the overall skill for the entire study area and contrast it against performance metrics defining forecast value (e.g., CO_2 emissions). The primary criterion for the chosen metric is that it has to be bounded to prevent skewed values upon aggregation, thus eliminating NSE $(-\infty, 1]$ as a candidate. As for the Pearson correlation coefficient, there is a possibility of positive and negative values cancelling each other out during the aggregation process, thus misleading both the strength and direction of the relationship between the actual and forecast time series. SMAPE is an accuracy metric that measures the difference between the actual and forecast data between 0 and 1, and is a metric that fulfills both requirements for our study. All candidate metrics are illustrated in Figure S2; across the reservoirs, forecast errors tend to be larger during the pre-monsoon (Feb-Apr). The skill then progressively increases until the end of the year. To derive the overall skill of a forecast member across space, we perform a weighted average of the errors with respect to the hydropower plant capacities following Eq. (4):

$$SMAPE_d = \sum_{i=1}^{N} (w_i * SMAPE_{i,d}), \tag{4}$$

where $SMAPE_d$ is the aggregated forecast error on day d, w_i is the weight of the i-th reservoir, taken as the hydropower capacity divided by the total capacity of the N reservoirs, and $SMAPE_{i,d}$ is the forecast error for the i-th reservoir on day d.

As for the forecast value, we consider six metrics: the available, dispatched, and unused hydropower, system operating costs, CO_2 emissions, and the number of N-1 violations—i.e., instances in which any of the high-voltage lines reaches 75% of its capacity—an indicator of grid stress. Here, note that the available hydropower is an output of the reservoir system model (derived through Eq. (2)), a commonly-used metric to assess forecast value in previous studies (Lee et al., 2022; Anghileri et al., 2019). The other metrics are produced by the power system model, and are thus chosen to represent multiple performance aspects of the grid. First, the hydropower metrics provide insights into how forecast value is transferred from the water system to the power system. Next, the system operating costs and CO_2 emissions provide insights into how system operations are impacted by different levels of forecast accuracy. Last, the N-1 violations indicate how stressed the transmission lines are. This is important, since (i) grid stress is considered one of the triggers for blackouts (Veloza & Santamaria, 2016), and (ii) can serve as an indicator of system performance (e.g., when line capacity limits the penetration of renewables in the grid (Chowdhury, Dang, et al., 2020)). In assessing the skill-value relationship, we note that there are other input variables (from both the reservoir and power system) that may influence the overall system performance. As such, besides forecast skill, the actual inflow (Q) and the electricity demand are also considered as system stressors.

5 Results

In this section, we first evaluate the benefits that lie in adopting streamflow forecasts when operating hydro-dominated power systems (Section 5.1). This is done by comparing results obtained from simulating the reservoir and power systems under different benchmark operating schemes. Then, we investigate how the value of forecasts changes with skill (Section 5.2). Here, we investigate the skill-value relationship under both standard operations (i.e., without feedback; Section 5.2.1) and operations with feedback between the power and water systems (Section 5.2.2). Such comparison illustrates how the value changes as we capture the interdependencies between water and power systems.

5.1 Value of streamflow forecasts

5.1.1 Comparison across multiple performance metrics

To determine the value of streamflow forecasts in power system operations, we aggregate the five key performance metrics across both space and time (since the reservoir model is run with a daily time-step and the power system model with an hourly time-step). The metrics include system-wide available and dispatched hydropower, system operating costs, CO_2 emissions, and number of N-1 violations (Figure 3). For comparison, we include the results for operations guided by rule curves and three different forecast-informed schemes, namely perfect forecasts, climatology, and the ensemble mean. At the monthly timescale, a strong seasonal pattern can be observed across all metrics. Despite the similar pattern exhibited by the different operating schemes, it is clear that the use of streamflow forecasts affects the operations of both reservoir and power system.

5.1.1.1 Available hydropower. Temporally, the system behavior can be classified into three periods, namely pre-monsoon (Feb-Apr), summer monsoon (May-Oct), and post-monsoon (Nov-Jan). The value of streamflow forecasts largely varies across these periods. We first focus on the amount of available hydropower, a direct product of the reservoir system model (boxplot in the top panel of Figure 3). Across all scenarios, the hydropower availability increases from the pre-monsoon to peak at the end of the monsoon, before decreasing again. This follows the seasonal pattern of the summer monsoon, a key feature of Southeast Asian climates (Chowdhury et al., 2021). Operating the reservoirs using rule curves results in larger hydropower availability than the schemes with forecasts during the pre-monsoon and monsoon period (see the corresponding mean and standard deviation in Table 2). During the monsoon, operating the dams without streamflow forecasts generates an average of at least 40 GWh more hydropower each month than the other schemes. This result is attributed to the nature of the decisions made with rule curves: without forecast, the release decisions of each reservoir are made with respect to the target storage only. As such, the reservoirs tend to release water whenever they receive large inflow volumes, resulting in large hydropower availability. Consequently, after the monsoon, the reduced inflow also causes the reservoirs to make smaller releases. The hydropower availability thus drops significantly (by 40–60% from November to December), averaging at least 60 GWh/month less than the forecast-informed schemes. In other words, this sharp decline is due to the myopic nature of the rule curves. In contrast, operating with forecasts allows the reservoirs to maintain a larger hydropower production after the monsoon. Looking at the specific forecast-informed schemes, we observe that operating with perfect foresight produces the best results throughout all seasons—a result that is consistent with past studies (Anghileri et al., 2019; Ahmad & Hossain, 2020; Doering et al., 2021; Guo et al., 2021; Lee et al., 2022).

5.1.1.2 Power-related metrics. The circles in the top panel of Figure 3 represent the hydropower dispatched within the grid. The first point to make is that not all available hydropower is dispatched by the grid. The mismatch between available and dispatched hydropower is accentuated during the monsoon season, when the amount of dispatched hy-

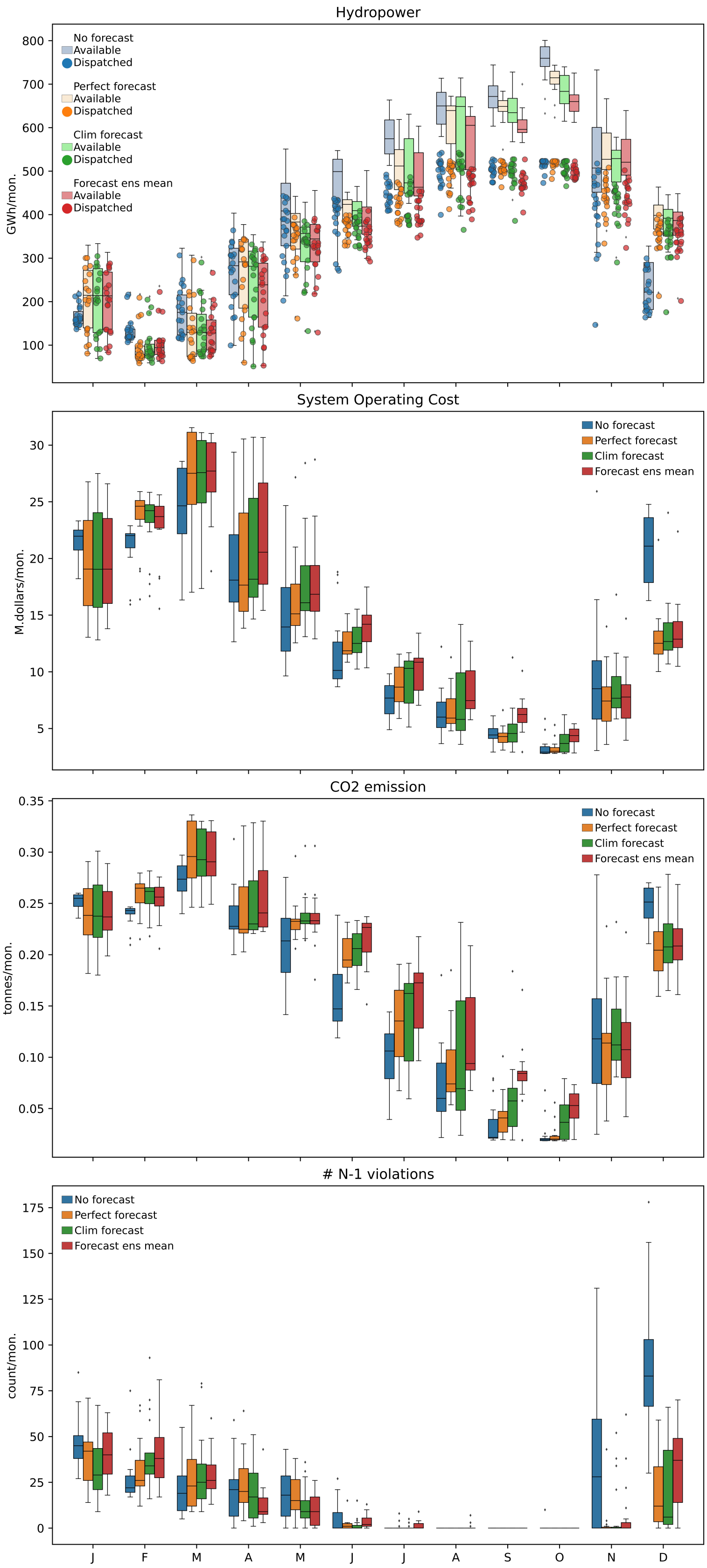

Figure 3. Monthly variability in system performance under different forecast-informed schemes. The four panels illustrate the range of variability in hydropower (available and dispatched), system operating costs, CO_2 emissions, and frequency of N-1 violations, respectively. All variables are spatially aggregated across the entire power system. Within each panel, the results from three forecast-informed schemes (perfect forecasts, climatology, and ensemble mean) are compared to the benchmark (no forecasts). Experiments are conducted without feedback between the reservoir and power systems.

Table 2. Variability in mean and standard deviation of the performance metrics illustrated in Figure 3 across different operating schemes (no forecasts, perfect forecasts, climatology and ensemble mean) and periods (pre-monsoon, monsoon and post-monsoon).

Performance metric	Scenario	Pre-monsoon	monsoon	Post-monsoon
Available hydropower (GWh/mon.)	No forecasts	195.16± 83.11	584.51±137.29	302.19±173.18
	Perfect forecasts	164.98±101.99	539.87±136.00	377.93±151.97
	Climatology	159.95± 91.11	527.80±142.82	360.75±142.47
	Ensemble mean	151.60± 78.62	506.85±132.20	366.82±146.94
Dispatched hydropower (GWh/mon.)	No forecasts	191.04± 76.31	451.26±71.55	267.27±120.78
	Perfect forecasts	160.62±94.75	439.50±76.23	329.83±114.60
	Climatology	157.17±86.50	431.12±82.74	319.20±111.61
	Ensemble mean	149.58±75.94	415.42±77.53	323.97±113.65
Unused hydropower (GWh/mon.)	No forecasts	4.12± 8.12	133.26± 69.40	34.92± 55.00
	Perfect forecasts	4.36± 8.57	100.37± 62.29	48.10± 40.90
	Climatology	2.78± 5.62	96.68± 62.58	41.54± 33.51
	Ensemble mean	2.02± 3.65	91.42± 56.61	42.85± 36.16
System operating cost (M.dollars/mon.)	No forecasts	21.58± 4.13	8.02± 4.70	17.28± 6.65
	Perfect forecasts	23.47± 5.21	8.67± 4.99	13.34± 5.91
	Climatology	23.68± 4.81	9.17± 5.39	13.99± 5.79
	Ensemble mean	24.16± 4.42	10.11± 5.12	13.70± 5.87
CO_2 emission (tonnes/mon.)	No forecasts	0.25± 0.02	0.10± 0.07	0.21± 0.07
	Perfect forecasts	0.27± 0.04	0.12± 0.08	0.18± 0.07
	Climatology	0.27± 0.03	0.13± 0.08	0.19± 0.06
	Ensemble mean	0.27± 0.03	0.14± 0.07	0.19± 0.07
# N-1 violations (hours/mon.)	No forecasts	22.96± 15.00	3.98± 9.32	59.16± 40.45
	Perfect forecasts	27.70± 15.67	3.39± 7.78	20.07± 21.10
	Climatology	30.00± 19.83	2.42± 6.13	20.65± 21.05
	Ensemble mean	27.63± 17.32	2.76± 5.42	26.21± 22.36

dropower not does not increase with hydropower availability. In fact, its value stabilizes around 450 GWh/month, leading to a larger discrepancy between the two metrics. This indicates a condition of over-production, a situation in which the grid is unable to dispatch all the available hydropower due to oversupply or limited transmission capacity. The percentage of total dispatched hydropower with respect to the total available for the four scenarios (no forecasts, perfect forecasts, climatology, and ensemble mean) over 19 years is 81.7%, 84.4%, 84.9%, and 85.1%, respectively. The discrepancy peaks at the end of the monsoon season, with up to 35%, 29%, 29%, and 28% of hydropower unused in the four scenarios, respectively. This indicates that defining value in terms of different performance metrics can produce varying conclusions. The current practice of defining value in terms of available hydropower (determined by a water system model), may therefore overlook the disparity between the available and dispatched hydropower, especially during the monsoon. To achieve a comprehensive understanding of streamflow forecast values, it is therefore important to evaluate the responses of multiple performance metrics spanning across water and power systems.

With the largest installed capacity in the grid (about 50%), hydropower fulfills more than half of the overall electricity demand in Cambodia. The amount of hydropower within the system thus plays a paramount role in determining the power system operations and the energy generation mix (refer to Figure S3 in the SI), which directly affects operating costs and CO_2 emissions. Referring to the second and third panel in Figure 3, an observation similar to the case of hydropower can be made; the benefits of operating with forecasts are accentuated during the post-monsoon season. Towards the end of the monsoon (in October), the scheme with perfect forecasts outperforms all other scenarios in terms of operating costs, and is comparable to the case without forecasts in terms of CO_2 emissions. This suggests that while the use of forecasts may not be very beneficial to the system during the pre-monsoon and the peak of the monsoon, given the right conditions, a better forecast can be advantageous from an earlier point in time to achieve lower operating costs and CO_2 emissions. A larger amount of hydropower in the grid also reduces stress in the transmission line, a point illustrated by the frequency of N-1 violations. There are, in particular, three transmission lines that are periodically stressed, two of which are part of a network that feeds Phnom Penh, Cambodia's capital and main load-centre (see Figure 1). The line congestions are eased as less pressure is placed on the thermal plants to fulfil the high demand. After the monsoon, the scenarios with forecasts are able to sustain the hydropower production, allowing more hydropower to be dispatched in the grid as opposed to the scenario without forecasts.

Given these results, it is evident that the use of streamflow forecasts is valuable to power system operations in terms of (i) reducing hydropower over-production during the monsoon, (ii) maintaining hydropower supply after the monsoon, and (iii) reducing transmission line stress. Importantly, these points are revealed by the use of a modelling framework accounting for both water and power system dynamics, something that would be hidden if one were to use a reservoir system model, thereby only focussing on the available hydropower. This highlights the complexity of the coupled water-energy system and the importance of exploring the multiple roles played by forecasts as we move beyond a water reservoir system.

5.1.2 Intra- and inter-annual variability of forecast value

Better understanding the inter- and intra-annual variability of forecast value can provide a deeper insight into when and why forecasts matter to grid operations in hydro-dominated power systems. To support this analysis, we focus solely on dispatched hydropower (which largely affects the power generation mix), and introduce a metric defined as the difference between the hydropower dispatched by each forecast-informed scheme and the one dispatched when adopting rule curves. Hence, positive values mean that a forecast-informed scheme performs better than rule curves. The values illustrated in Figure 4 reveal a few interesting insights. First, the benefit associated to forecasts is most of the time negative between February and October, meaning that forecasts are in general not beneficial during the pre-monsoon and monsoon seasons. This is in contrast to the period between November and January (post-monsoon season), when positive benefits are observed. Second, positive benefits extend to almost 200 GWh/month, while the negative ones to less than -100 GWh/month. This indicates that the extent of benefits derived from using forecast-informed schemes, albeit less frequent, is more significant. Third, there are a few instances in which positive benefits are observed during the the pre-monsoon and monsoon seasons (e.g., April 2007, June 2010, July 2004). These episodes are due to specific, and unexpected, fluctuations in dam inflow for that particular year. In 2007, for instance, the 30-day outlook shows that the inflow will keep increasing in May, therefore the reservoirs release more water and produce more hydropower, which is then dispatched into the grid (refer to Figure S4 in the SI). This information is unknown to the scheme without forecast, explaining the larger benefits derived in April 2007.

Looking at the inter-annual variability, our results show that the three best and worst performing years are 2000, 2001, 2018, and 2002, 2005, and 2008, respectively. A closer look at the reservoir inflow corresponding to each year, shown in Figure 5, gives us two insights regarding the hydrological conditions that are favorable to forecast-informed schemes. First, larger inflow volumes tend to be beneficial. Second, and perhaps more interesting, forecasts are more useful when the inflow patterns present sudden and unexpected changes; a situation that can be hardly managed when controlling a reservoir system with rule curves.

5.2 Skill-value relationship

To understand how forecast value changes with skill, we conducted deterministic simulations using the 11 individual streamflow forecast members. We then investigate the skill-value relationship under two reservoir operating schemes: (i) without (Section 5.2.1) and (ii) with (Section 5.2.2) feedback between the reservoir and power systems. This allows us to characterize the skill-value relationship under different levels of integration of the coupled water-energy system.

5.2.1 System operations without feedback

To study the relationship between forecast skill and value, we define skill using the forecast error (Section 4) and relate it to difference performance metrics that characterize forecast value, namely available, dispatched, and unused hydropower, system operating costs, CO_2 emissions, and number of N-1 violations. In our analysis, we also consider two additional variables, or stressors, that may affect system performance. These are the inflow to the reservoirs and electricity demand, or load. All these variables are then analyzed through a correlation matrix and a multiple linear regression model, whose results are reported Figure 6.

Beginning with the correlation analysis (left panel), our results show that the correlation between stressors and performance is significant ($p < 0.05$) for most stressor-metric pairs. Beginning with the forecast error, we note two important patterns. First, there is a strong negative correlation between error and available and dispatched hydropower, meaning that, as the error increases, the contribution of hydropower to the generation mix decreases. In turn, this explains the positive correlation with costs, CO_2 emissions, and N-1 violations (recall that the power system must rely more on thermoelectric power and imports when less hydropower is available). Second, the strength of the relationship between forecast error and performance metrics decreases as we move from the reservoir system to the power system, a result that is explained by the fact that other stressors become relevant when studying coupled water-energy systems. Inflow, for instance, positively affects hydropower-related and negatively affects costs, CO_2 emissions, and grid stress. An increase in load, on the other hand, implies an increase in costs and CO_2 emissions.

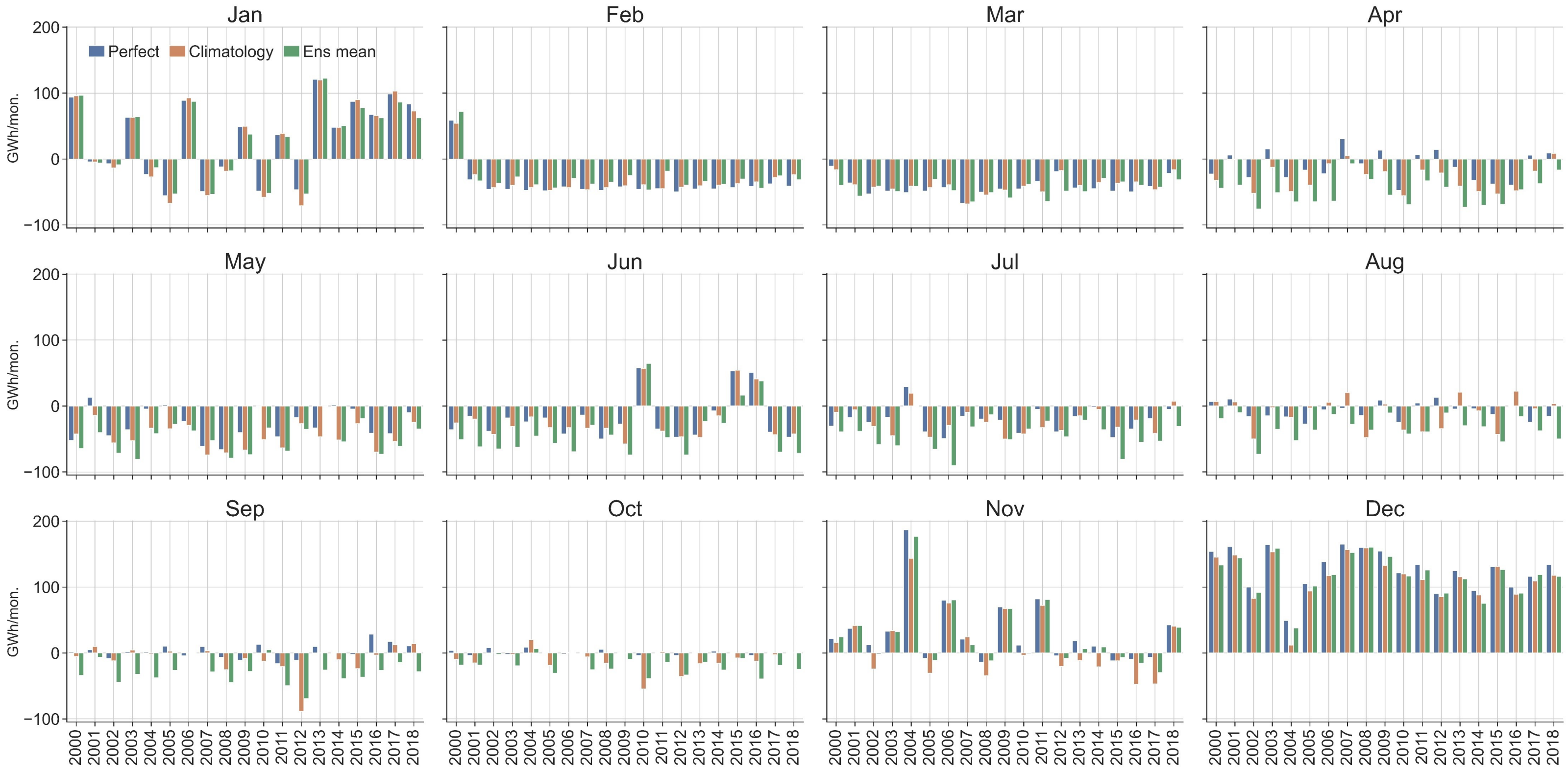

Figure 4. Benefit of using streamflow forecasts at different times of the year, defined as the difference between the amount of hydropower dispatched with and without forecast. The results are grouped according to calendar months (12 panels) and year (horizontal axis). Each cluster of three bars represents the three forecast-informed schemes: perfect forecasts, climatology, and ensemble mean. The values shown are the positive/negative benefits of using each kind of forecast, i.e., the difference between the hydropower dispatched by each forecast-informed scheme and the one dispatched when adopting rule curves.

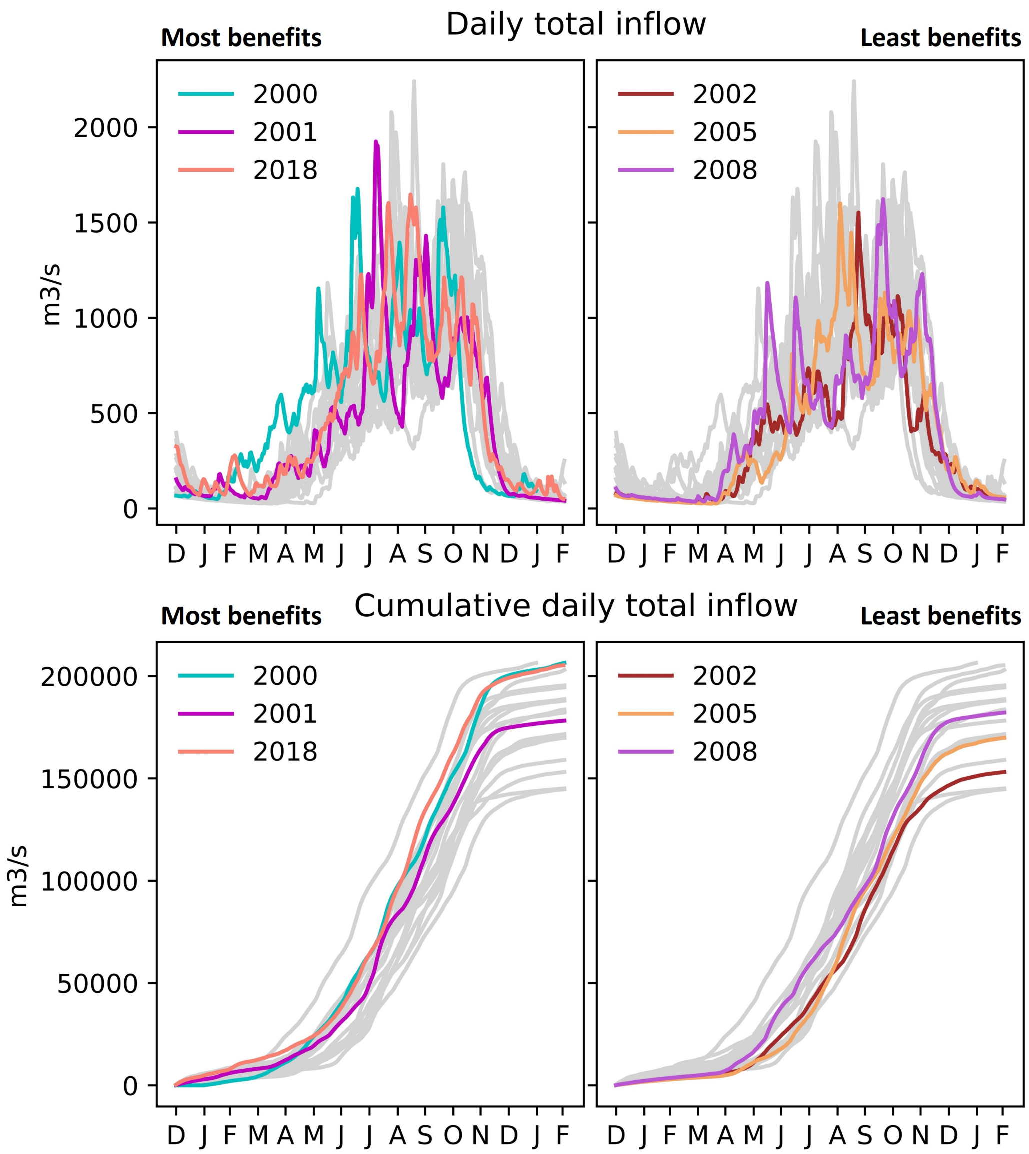

Figure 5. Comparison of daily time series (top panels) and cumulative (bottom panels) inflow profiles across different years. Each gray line represents one year between 2000 and 2018. Based on the total hydropower dispatched each year, three years with the highest and lowest benefits are identified and highlighted in the left and right panels, respectively.

To further understand how forecast error, inflow, and load control the performance metrics, we identify multiple linear regression models in which the inputs are the significant independent variables (predictors) and each of the six metrics are the dependent variables (predictands). All variables are first standardized (by subtracting the variable's mean from each observed value and then dividing by the variable's standard deviation) to facilitate the comparison. Using a forward selection approach, the predictors are iteratively added to the regression model, beginning from the one with the highest (absolute value of) correlation coefficient r (Galelli, Humphrey, et al., 2014). From the model, the coefficient of determination (r^2) and final regression coefficients allow us to infer the contribution of each predictor to the variance of the predictands, and hence the importance of the model inputs. The variables are grouped according to the calendar months before carrying out the regression. The results are illustrated in the central and right panels of Figure 6.

Similar to the previous analyses, this analysis can also be organized around three periods, i.e., pre-monsoon, monsoon and post-monsoon. The importance of the forecast error for the available hydropower is more obvious during the post-monsoon season, since a discrepancy between observed and predicted inflow determines how well the system can adapt to foreseen changes in reservoir inflow and overall transition into the dry season. This is in contrast to the monsoon season, when the reservoirs usually release close to the maximum designed release, reducing the importance of forecast errors. Moving to the next metric, the dispatched hydropower is determined through power system operations. During the pre-monsoon, less hydropower is produced, and whatever is produced usually gets fully utilized. The importance of inflow and error to hydropower usage is thus similar to that of hydropower production between February and April. During the monsoon, however, the abundant hydropower production forces the electricity demand to be the limiting factor for the amount of dispatched hydropower, explaining the importance of load during this period. Regardless of the error or inflow, the power system constraints dictate the grid usage. The dynamics between the available and dispatched hydropower also directly influence the next metric, i.e., the unused hydropower. As seen from the regression coefficients, a reduction in load can create a more than proportionate increase in the amount of unused hydro. The over-production peaks in October across all forecast-informed schemes, with about 30% unused hydro. Figure 6 also suggests that the forecast errors become insignificant beyond the first two performance metrics, since the power system performance depends primarily on inflow and load.

Breaking down the relative contributions of forecast errors, reservoir inflow, and electricity demand to different performance metrics highlights the complexity of the systems and the interdependencies between stressors. Streamflow forecasts are most valuable to improving power system performance during the post-monsoon by facilitating a smooth transition between the monsoon and post-monsoon seasons. A more accurate forecast allows resources to be exploited for continued hydropower availability for the grid to dispatch. As we move from the water system to the power system, the skill-value relationship becomes less significant, as the system responses depend more on the electricity demand.

5.2.2 System operations with feedback

The operations of the reservoir and power systems may not be entirely independent. To characterize the skill-value relationship under a tighter integration of the two systems, we repeat all experiments with the same inputs, but this time adding the feedback between the power and reservoir systems. This set of experiments thus makes use of the re-operation module described in Section 3.4. Using the same methodology described in Section 5.2.1, we study the relationship between the system stressors and performance metrics illustrated in Figure 7.

With the re-operation mechanism in place, the role played by electricity demand is amplified, while the importance of forecast skill (error) and reservoir inflow is largely reduced.

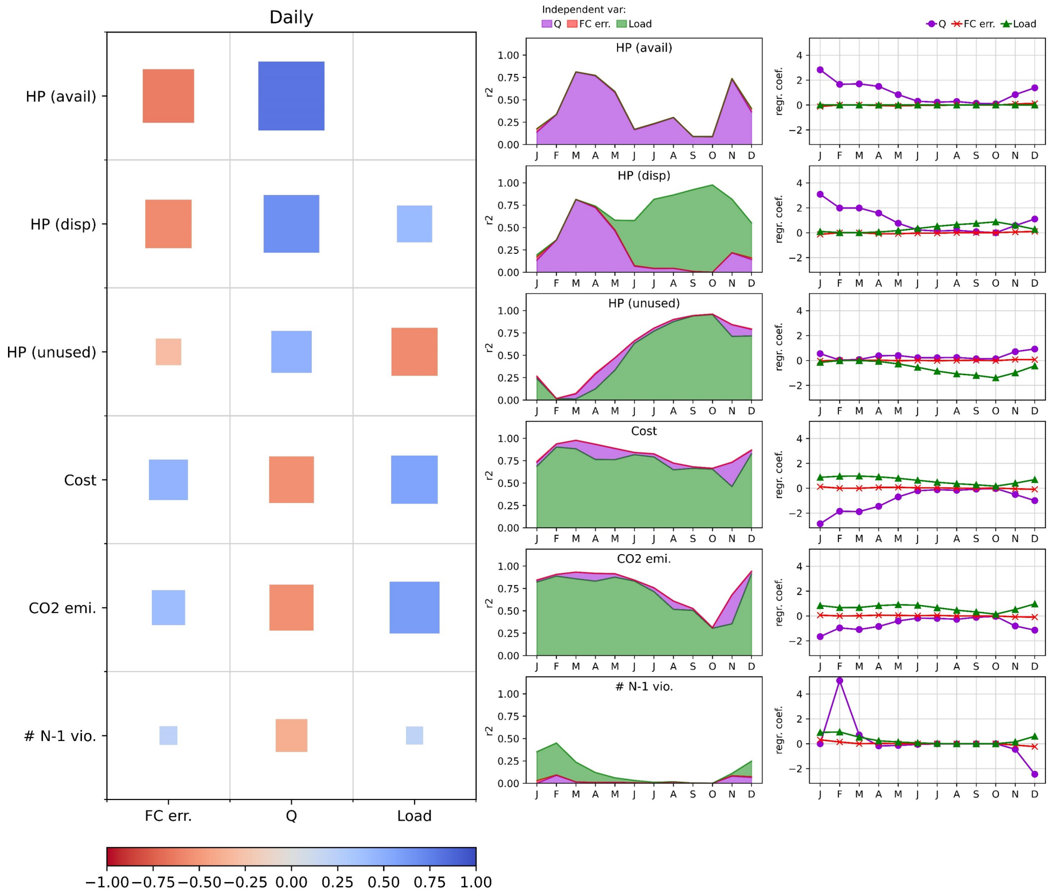

Figure 6. Relationship between system stressors (forecast error, inflow, and load) and performance metrics (available, dispatched, and unused hydropower, system operating costs, CO_2 emissions, and number of N-1 violations) illustrated by a correlation matrix (left) and regression model results (center and right). In the correlation matrix, the values (shown in the color bar) between each stressor-metric pair are obtained by bootstrapping the data through 1,000 iterations. Based on the correlation values, we first identify a multiple linear regression model between the stressors (predictors) and metrics (predictands), and then estimate the contribution of each predictor to the explained variance (center) and the corresponding regression coefficients (right). These results are reported for the scenarios that do not include the feedback between the power and water system.

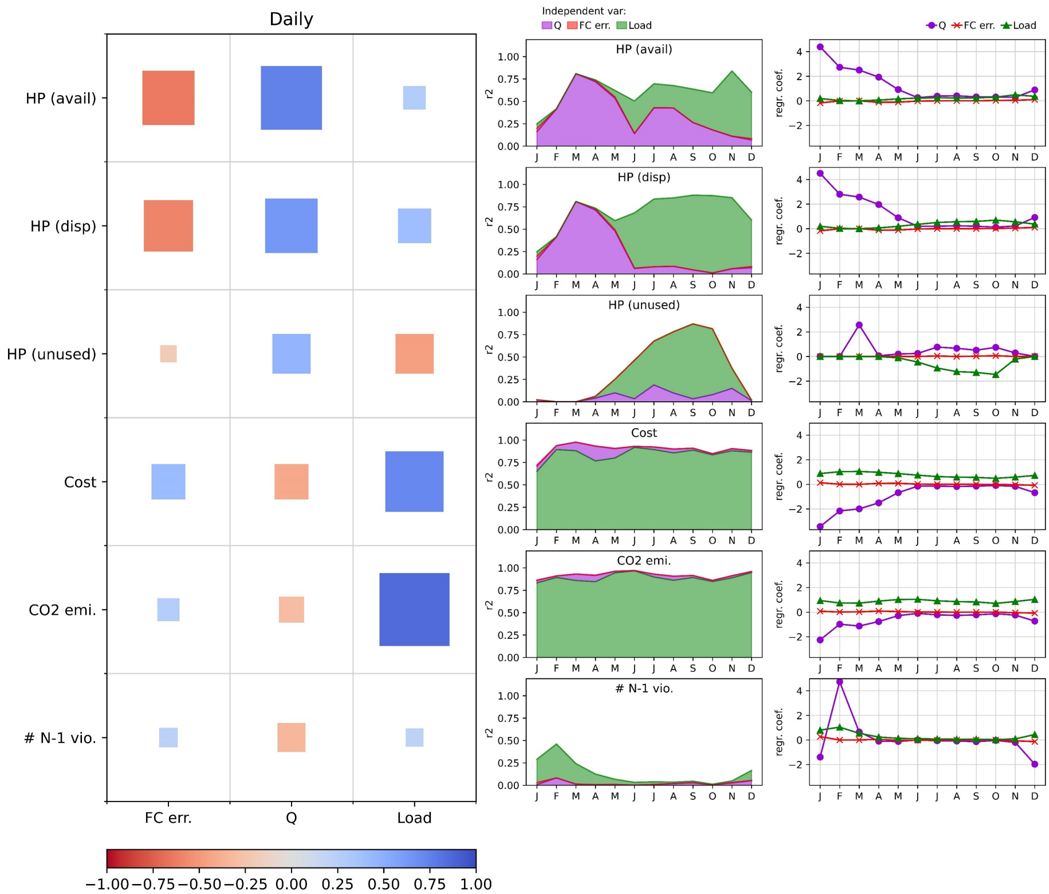

Figure 7. Relationship between system stressors (forecast error, inflow, and load) and performance metrics (available, dispatched, and unused hydropower, system operating costs, CO_2 emissions, and number of N-1 violations). These results are reported for the scenarios that include the feedback between the power and water system.

As the goal of the re-operation mechanism is to flexibly store and release water to generate hydropower that better matches the power system demand, the reservoir storage patterns can largely deviate from the seasonal patterns (Koh et al., 2022). In turn, this partially dampens the impact of hydrological variability on power system performance, making both inflow and forecast skill less important. With hydropower-related metrics being explained by load, it follows that operating costs and CO_2 emissions can almost entirely be determined by load as well, with r^2 values close to one for every month. Evidently, the presence of the feedback mechanism reduces the value of forecasts, allowing load to dominate the operating decisions in both the reservoirs and power system.

6 Discussion and conclusions

Our study evaluates the value of streamflow forecasts in hydro-dominated power systems. The performance metrics were selected from both the reservoir and power systems to represent the hydropower generation by the reservoirs, hydropower usage within the grid, as well as economic, environmental, and reliability aspects of the power system. We show that defining forecast value in terms of different performance metrics can produce different outcomes. For instance, while previous studies often associate favorable forecasts with greater hydropower availability, we found that larger hydropower availability does not necessarily translate into more usage within the grid. Unless the excess water release can serve a second purpose—such as for groundwater storage (Nayak et al., 2018) or inter-basin transfer (Li et al., 2014)—measuring value only in terms of the available hydropower may thus overlook other important aspects, such as production costs or CO_2 emissions. Therefore, when we study hydropower systems, we should consider the role that hydropower reservoirs play, not only within the reservoir network, but also within the power system as well.

In hydro-dominated power systems, hydropower operations are highly influenced by the seasonality of reservoir inflow. As a result, the grid operations and performance exhibit a strong seasonal profile as well. In our case study, the system behavior can be classified into three periods—pre-monsoon, monsoon and post-monsoon. We show that the value of streamflow forecasts varies with these different periods. During the monsoon, the use of forecasts reduces hydropower over-production. In the post-monsoon season, operating with forecasts is beneficial to sustain hydropower supply. Accurate forecasts are especially useful during the three months after the end of the monsoon to facilitate the transition from wet to dry seasons. Better forecast skill, combined with large inflow conditions, can thus benefit the system in terms of larger dispatched hydropower, lowering operating costs and CO_2 emissions. Our analysis also shows that, with a tighter integration of the reservoir and power systems, the role played by electricity demand becomes dominant in determining operational decisions within both systems.

Looking forward, an important aspect warranting additional research is the impact of the uncertainty associated to streamflow forecasts, which could be 'operationalized' through the use of stochastic MPC schemes (Pianosi & Soncini-Sessa, 2009). Such control schemes would become particularly useful when dealing with streamflow forecasts spanning across longer timescales than those currently available for this region. Another relevant aspect to consider in the future is the integration of other forms of forecasts that could improve the operation of water-energy systems, such as electric load forecasts (Hong & Fan, 2016).

Overall, we believe that a better understanding of the value provided by streamflow forecasts to multi-sector infrastructures could promote and support their use. The need for better approaches to system operations is indeed necessary in a variety of contexts, from regions experiencing hydro-climatological shifts to regions, like Southeast Asia, that are expanding their water and power supply networks.

Notation

$\boldsymbol{S_d^i}$ Storage on day d of the i-th reservoir
$\boldsymbol{S_{cap}^i}$ Capacity of the i-th reservoir
$\boldsymbol{R_d^i}$ Volume of water released through the turbines of the i-th reservoir on day d
$\boldsymbol{R_{max}^i}$ Maximum volume of water that can be turbined from the i-th reservoir
$\boldsymbol{Q_d^i}$ Inflow on day d to the i-th reservoir
$\boldsymbol{Q_{MEF,d}^i}$ Downstream environmental flow requirement of the i-th reservoir on day d
$\boldsymbol{spill_d^i}$ Volume of water spilled from the i-th reservoir on day d
$\boldsymbol{E_d^i}$ Evaporation losses from the i-th reservoir on day d
$\boldsymbol{HP_d^i}$ Available hydropower on day d from the i-th reservoir
$\boldsymbol{HP_t^{i*}}$ Hydropower dispatched in hour t from the i-th reservoir
$\boldsymbol{H_d^i}$ Hydraulic head from the i-th reservoir on day d

Open Research Section

The data and Python scripts used to simulate the water-energy system in Cambodia for this research are available at Koh (2023) via `https://doi.org/10.5281/zenodo.8163034`.

The observed reservoir inflow data are available from `https://doi.org/10.24381/cds.a4fdd6b9` (Harrigan et al., 2021) and the reservoir inflow forecast data are available from `https://doi.org/10.24381/cds.2d78664e` (Zsoter et al., 2020). Power system parameters, including generator and transmission line specifications, as well as monthly electricity peak demand data are extracted from EDC (2016) and JICA (2014).

Acknowledgments

Rachel Koh is supported by the President's Graduate Fellowship from the Singapore University of Technology and Design.

References

Ahmad, S., & Hossain, F. (2020). Maximizing energy production from hydropower dams using short-term weather forecasts. *Renewable Energy*, *146*, 1560–1577.

Anghileri, D., Monhart, S., Zhou, C., Bogner, K., Castelletti, A., Burlando, P., & Zappa, M. (2019). The value of subseasonal hydrometeorological forecasts to hydropower operations: How much does preprocessing matter? *Water Resources Research*, *55*(12), 10159–10178.

Anghileri, D., Voisin, N., Castelletti, A., Pianosi, F., Nijssen, B., & Lettenmaier, D. (2016). Value of long-term streamflow forecasts to reservoir operations for water supply in snow-dominated river catchments. *Water Resources Research*, *52*(6), 4209–4225.

Chowdhury, A. K., Dang, T. D., Bagchi, A., & Galelli, S. (2020). Expected benefits of Laos' hydropower development curbed by hydroclimatic variability and limited transmission capacity: Opportunities to reform. *Journal of Water Resources Planning and Management*, *146*(10), 05020019.

Chowdhury, A. K., Dang, T. D., Nguyen, H., Koh, R., & Galelli, S. (2021). The Greater Mekong's climate-water-energy nexus: How ENSO-triggered regional droughts affect power supply and CO_2 emissions. *Earth's Future*, *9*(3).

Chowdhury, A. K., Kern, J., Dang, T. D., & Galelli, S. (2020). PowNet: A network-constrained unit commitment/economic dispatch model for large-scale power systems analysis. *Journal of Open Research Software*, *8*(1).

Dang, T. D., Vu, D. T., Chowdhury, A. K., & Galelli, S. (2020). A software package for the representation and optimization of water reservoir operations in the VIC hydrologic model. *Environmental Modelling and Software*, *126*.

Delaney, C., Hartman, R., Mendoza, J., Dettinger, M., Delle Monache, L., Jasperse, J., ... Evett, S. (2020). Forecast informed reservoir operations using ensemble streamflow predictions for a multipurpose reservoir in Northern California. *Water Resources Research*, *56*(9), e2019WR026604.

Ding, Z., Wen, X., Tan, Q., Yang, T., Fang, G., Lei, X., ... Wang, H. (2021). A forecast-driven decision-making model for long-term operation of a hydro-wind-photovoltaic hybrid system. *Applied Energy*, *291*, 116820.

Doering, K., Quinn, J., Reed, P., & Steinschneider, S. (2021). Diagnosing the time-varying value of forecasts in multiobjective reservoir control. *Journal of Water Resources Planning and Management*, *147*(7), 04021031.

EDC. (2016). *Annual Report 2016* (Tech. Rep.). Electricité du Cambodge (EDC).

Galelli, S., Dang, T. D., Ng, J. Y., Chowdhury, A. K., & Arias, M. E. (2022). Opportunities to curb hydrological alterations via dam re-operation in the mekong. *Nature Sustainability*, *5*(12), 1058–1069.

Galelli, S., Goedbloed, A., Schwanenberg, D., & van Overloop, P. (2014). Optimal real-time operation of multipurpose urban reservoirs: Case study in Singapore. *Journal of Water Resources Planning and Management*, *140*(4), 511–523.

Galelli, S., Humphrey, G. B., Maier, H. R., Castelletti, A., Dandy, G. C., & Gibbs, M. S. (2014). An evaluation framework for input variable selection algorithms for environmental data-driven models. *Environmental Modelling & Software*, *62*, 33–51.

Gebretsadik, Y., Fant, C., Strzepek, K., & Arndt, C. (2016). Optimized reservoir operation model of regional wind and hydro power integration case study: Zambezi basin and South Africa. *Applied Energy*, *161*, 574–582.
Gong, Y., Liu, P., Ming, B., & Li, D. (2021). Identifying the effect of forecast uncertainties on hybrid power system operation: A case study of Longyangxia hydro–photovoltaic plant in China. *Renewable Energy*, *178*, 1303–1321.
Grantz, K., Rajagopalan, B., Clark, M., & Zagona, E. (2005). A technique for incorporating large-scale climate information in basin-scale ensemble streamflow forecasts. *Water Resources Research*, *41*(10).
Guo, Y., Xu, Y., Xie, J., Chen, H., Si, Y., & Liu, J. (2021). A weights combined model for middle and long-term streamflow forecasts and its value to hydropower maximization. *Journal of Hydrology*, *602*, 126794.
Harrigan, S., Zsoter, E., Barnard, C., Wetterhall, F., Ferrario, I., Mazzetti, C., ... Prudhomme, C. (2021). *River discharge and related historical data from the Global Flood Awareness System, v3.1, Copernicus Climate Change Service (C3S) Climate Data Store (CDS).* Retrieved from `https://doi.org/10.24381/cds.a4fdd6b9`
Hong, T., & Fan, S. (2016). Probabilistic electric load forecasting: A tutorial review. *International Journal of Forecasting*, *32*(3), 914–938.
Huang, Z., & Zhao, T. (2022). Predictive performance of ensemble hydroclimatic forecasts: Verification metrics, diagnostic plots and forecast attributes. *Wiley Interdisciplinary Reviews: Water*, *9*(2), e1580.
Ibanez, E., Magee, T., Clement, M., Brinkman, G., Milligan, M., & Zagona, E. (2014). Enhancing hydropower modeling in variable generation integration studies. *Energy*, *74*, 518–528.
JICA. (2014). *Preparatory survey for Phnom Penh city transmission and distribution system expansion project phase II in the Kingdom of Cambodia* (Tech. Rep.). Japan International Cooperation Agency (JICA).
Kern, J. D., Su, Y., & Hill, J. (2020). A retrospective study of the 2012–2016 California drought and its impacts on the power sector. *Environmental Research Letters*, *15*(9).
Koh, R. (2023). PowNetRes_FC: Initial release (v1.0). Zenodo. [Dataset and Software]. Retrieved from `https://doi.org/10.5281/zenodo.8163034`
Koh, R., Kern, J., & Galelli, S. (2022). Hard-coupling water and power system models increases the complementarity of renewable energy sources. *Applied Energy*, *321*, 119386.
Lee, D., Ng, J., Galelli, S., & Block, P. (2022). Unfolding the relationship between seasonal forecast skill and value in hydropower production: A global analysis. *Hydrology and Earth System Sciences*, *26*(9), 2431–2448.
Li, W., Sankarasubramanian, A., Ranjithan, R., & Brill, E. (2014). Improved regional water management utilizing climate forecasts: An interbasin transfer model with a risk management framework. *Water Resources Research*, *50*(8), 6810–6827.
Lima, C., & Lall, U. (2010). Climate informed monthly streamflow forecasts for the Brazilian hydropower network using a periodic ridge regression model. *Journal of hydrology*, *380*(3–4), 438–449.
Liu, P., Guo, S., Xu, X., & Chen, J. (2011). Derivation of aggregation-based joint operating rule curves for cascade hydropower reservoirs. *Water Resources Management*, *25*, 3177–3200.
MacLeod, D., Easton-Calabria, E., de Perez, E., & Jaime, C. (2021). Verification of forecasts for extreme rainfall, tropical cyclones, flood and storm surge over Myanmar and the Philippines. *Weather and climate extremes*, *33*, 100325.
McInerney, D., Thyer, M., Kavetski, D., Laugesen, R., Tuteja, N., & Kuczera, G. (2020). Multi-temporal hydrological residual error modeling for seamless subseasonal streamflow forecasting. *Water Resources Research*, *56*(11), e2019WR026979.
Nash, J. E., & Sutcliffe, J. V. (1970). River flow forecasting through conceptual models part I—A discussion of principles. *Journal of hydrology*, *10*(3), 282–290.
Nayak, M., Herman, J., & Steinschneider, S. (2018). Balancing flood risk and water supply

in California: Policy search integrating short-term forecast ensembles with conjunctive use. *Water Resources Research*, *54*(10), 7557–7576.

Ogliari, E., Guilizzoni, M., Giglio, A., & Pretto, S. (2021). *Renewable Energy*, *178*, 1466–1474.

Oliveira, R., & Loucks, D. (1997). Operating rules for multireservoir systems. *Water Resources Research*, *33*(4), 839–852.

Pastor, A. V., Ludwig, F., Biemans, H., Hoff, H., & Kabat, P. (2014). Accounting for environmental flow requirements in global water assessments. *Hydrology and Earth System Sciences*, *18*(12), 5041–5059.

Pianosi, F., & Soncini-Sessa, R. (2009). Real-time management of a multipurpose water reservoir with a heteroscedastic inflow model. *Water Resources Research*, *45*(10).

Quedi, E., & Fan, F. (2020). Sub seasonal streamflow forecast assessment at large-scale basins. *Journal of Hydrology*, *584*, 124635.

Slater, L. J., Villarini, G., Bradley, & A., A. (2016). Evaluation of the skill of north-American multi-model ensemble (NMME) global climate models in predicting average and extreme precipitation and temperature over the continental USA. *Climate Dynamics*, *53*, 7381-–7396.

Soncini-Sessa, R., Weber, E., & Castelletti, A. (2007). *Integrated and participatory water resources management-theory.* Amsterdam, The Netherlands: Elsevier.

Troin, M., Arsenault, R., Wood, A. W., Brissette, F., & Martel, J.-L. (2021). *Generating ensemble streamflow forecasts: A review of methods and approaches over the past 40 years* (Vol. 56) (No. 7). Wiley Online Library.

Turner, S., Bennett, J. C., Robertson, D. E., & Galelli, S. (2017). Complex relationship between seasonal streamflow forecast skill and value in reservoir operations. *Hydrology and Earth System Sciences*, *21*(9), 4841–4859.

Turner, S., Xu, W., & Voisin, N. (2020). Inferred inflow forecast horizons guiding reservoir release decisions across the United States. *Hydrology and Earth System Sciences*, *24*(3), 1275-1291.

Veloza, O., & Santamaria, F. (2016). Analysis of major blackouts from 2003 to 2015: Classification of incidents and review of main causes. *The Electricity Journal*, *29*(7), 42–49.

Voisin, N., Dyreson, A., Fu, T., O'Connell, M., Turner, S. W., Zhou, T., & Macknick, J. (2020). Impact of climate change on water availability and its propagation through the Western US power grid. *Applied Energy*, *276*, 115467.

Voisin, N., Hamlet, A. F., Graham, L. P., Pierce, D. W., Barnett, T. P., & Lettenmaier, D. P. (2006). The role of climate forecasts in Western U.S. power planning. *Journal of Applied Meteorology and Climatology*, *45*(5), 653–673.

Wang, F., Wang, L., Zhou, H., Saavedra Valeriano, O., Koike, T., & Li, W. (2012). Ensemble hydrological prediction-based real-time optimization of a multiobjective reservoir during flood season in a semiarid basin with global numerical weather predictions. *Water Resources Research*, *48*(7).

Yassin, F., Razavi, S., Elshamy, M., Davison, B., Sapriza-Azuri, G., & Wheater, H. (2019). Representation and improved parameterization of reservoir operation in hydrological and land-surface models. *Hydrol. Earth Syst. Sci.*, *23*(9), 3735–3764.

Yossef, N., Winsemius, H., Weerts, A., van Beek, R., & Bierkens, M. (2013). Skill of a global seasonal streamflow forecasting system, relative roles of initial conditions and meteorological forcing. *Water Resources Research*, *49*(8), 4687–4699.

Zhao, T., Yang, D., Cai, X., Zhao, J., & Wang, H. (2012). Identifying effective forecast horizon for real-time reservoir operation under a limited inflow forecast. *Water Resources Research*, *48*(1).

Zimmerman, B., Vimont, D., & Block, P. (2016). Utilizing the state of ENSO as a means for season-ahead predictor selection. *Water Resources Research*, *52*(5), 3761–3774.

Zsoter, E., Harrigan, S., Barnard, C., Blick, M., Ferrario, I., Wetterhall, F., & Prudhomme, C. (2020). *Reforecasts of river discharge and related data by the Global Flood Awareness System, v2.2, Copernicus Climate Change Service (C3S) Climate Data Store*

(CDS). Retrieved from https://doi.org/10.24381/cds.2d78664e

Evaluating Streamflow Forecasts in Hydro-Dominated Power Systems–When and Why They Matter

Rachel Koh [1], Stefano Galelli [1,2]

[1]Pillar of Engineering Systems and Design, Singapore University of Technology and Design, Singapore
[2]School of Civil and Environmental Engineering, Cornell University, Ithaca, NY

Key Points:

- The benefits of streamflow forecasts trickle down from the water to the power system
- Forecasts are particularly useful during the transition from wet to dry seasons
- The relationship between forecast skill-value is controlled by the level of operational integration between the two systems

Corresponding author: Rachel Koh, kohzq.rachel@gmail.com

Abstract

The value of seasonal streamflow forecasts for the hydropower industry has long been assessed by considering metrics related to hydropower availability. However, this approach overlooks the role played by hydropower dams within the power grid, therefore providing a myopic view of how forecasts could improve the operations of large-scale power systems. With the aim of understanding how the value of streamflow forecasts penetrates through the power grid, we developed a coupled-water energy model that is subject to reservoir inflow forecasts with different levels of accuracy. We implement the modelling framework on a real-world case study based on the Cambodian grid, which relies on hydropower, coal, oil, and imports from neighboring countries. In particular, we evaluate the performance in terms of metrics selected from both the reservoir and power systems, including available and dispatched hydropower, power production costs, CO_2 emissions, and transmission line congestion. Through this framework, we demonstrate that streamflow forecasts can positively impact the operations of hydro-dominated power systems, especially during the transition from wet to dry seasons. Moreover, we show that the value largely varies with the specific metric of performance at hand as well as the level of operational integration between water and power systems.

Plain Language Summary

Forecasts of river streamflow are regularly used by water system operators to plan the operations of large-scale infrastructures, such as hydropower dams. To date, research has focussed primarily on how the accuracy, or skill, of forecasts translates into added performance of reservoir systems, thereby overlooking the potential benefits for other interconnected infrastructures that depend on water availability. Here, we focus on the case on national power grids, whose performance is partially controlled by hydropower production. We show that the use of streamflow forecasts could bring benefits that 'trickle down' to power system operations, reducing, for instance, power production costs and CO_2 emissions during specific periods.

1 Introduction

Water managers often rely on streamflow forecasts to inform reservoir release decisions (Turner et al., 2020). As opposed to operating reservoir networks with static rule curves, streamflow forecasts offer operators the ability to dynamically adapt to anticipated inflow conditions (Troin et al., 2021). Accurate streamflow forecasts have been found to benefit multiple aspects of water management, such as flood control, water supply reliability, or hydropower production (Nayak et al., 2018; Delaney et al., 2020). The metrics used to assess the benefits, or value, of streamflow forecasts can be broadly classified under two categories. Under the first category, benefits are defined in terms of deviations from a predefined target, usually the target storage or release (Li et al., 2014; Turner et al., 2017). Under the second category, benefits are defined through metrics measuring the improvement in performance with respect to one or multiple objectives. Examples include reduction in water shortage (Nayak et al., 2018) or spilled water volume (Anghileri et al., 2016), better flood control (Wang et al., 2012; Galelli, Goedbloed, et al., 2014), and hydropower generation or revenue (Anghileri et al., 2019; Ahmad & Hossain, 2020; Doering et al., 2021; Guo et al., 2021; Lee et al., 2022). The common denominator among these metrics is that they are based on the output produced by a reservoir system model.

In hydro-dominated power systems, reservoir operations can have profound effects on power system operations (Voisin et al., 2020; Chowdhury et al., 2021; Chowdhury, Dang, et al., 2020). During dry conditions, for instance, a decrease in hydropower production may force power grid operators to raise production from thermoelectric plants, leading to higher operating costs and CO_2 emissions (Kern et al., 2020; Chowdhury et al., 2021). Defining streamflow forecast value solely in terms of water-related metrics thus overlooks the role played by hydropower reservoirs in the power grid. In this regard, it is worth stressing that there are only a handful of studies that evaluated whether the use of streamflow forecasts brings value to power grid operations (Ding et al., 2021; Gong et al., 2021). Both studies were conducted at the scale of a river basin—rather than on a spatial domain encompassing a national or regional grid—and adopted performance metrics defined in terms of power production only (i.e., supply from hydropower, wind, and solar photovoltaic). Hence, an in-depth understanding of how power system operations could benefit of streamflow forecasts is missing. In particular, it is important to understand which performance metrics are improved by the use of streamflow forecasts, when forecasts are most useful, and how forecast skill translates into different performance metrics. All these aspects would indeed be relevant to support the operationalization of streamflow forecasts.

Here, we aim to advance the current body of knowledge by studying how the value of streamflow forecasts unfolds as we move beyond a water reservoir system to include the operations of a national power grid. The questions of interest are therefore the following: How does forecast value change as we consider different performance aspects of a power grid? When is the use of forecasts more beneficial? How does forecast skill affect power system operations? Is forecast value affected by the interdependencies of the water-energy system? With the aid of a reservoir and power system model, we answer these questions by evaluating the value of streamflow forecasts for the operations of the Cambodian power system, which largely relies on the hydropower sector (Section 2 and 3). The criteria used in such evaluation are multiple metrics taken from both the reservoir and power systems, including available hydropower, dispatched hydropower (i.e., hydropower used within the grid), power production costs, CO_2 emission, and transmission line stress (Section 4). By simulating the coupled water-energy system with and without streamflow forecasts, we show that forecasts are particularly useful during the transition from the summer monsoon to the dry season. We also quantify the relationship between forecast skill and value, and show that forecast error is less important for production costs and CO_2 emissions, which are also impacted by electricity demand. We finally study how different levels of integration between water and power systems reshapes the skill-value relationship (Section 5).

2 Case study and Data

2.1 Case study

We carried out our analysis on the Cambodian water-energy system, illustrated in Figure 1. The representation of the system is based on the infrastructure built and operated in 2016, for which detailed data are available (Chowdhury, Kern, et al., 2020). Power supply is largely controlled by a network of six hydropower dams, which have a total installed capacity of 1,048 MW (see Table 1). In this reservoir network, there are two embankment dams (Kirirom I and Kirirom III), two dams operated in cascade (Atay and LR Chrum), and two headwater dams (Kamchay and Tatay). As we shall see, their production shows a pronounced inter-annual pattern; production increases during the summer monsoon (typically between May and October) and decreases during the dry season. The hydropower production is complemented by a few additional resources, namely thermoelectric plants (three coal-fired units totaling 400 MW of installed capacity and 15 oil-fired units totaling 282 MW), and import from neighboring countries (Thailand, Laos, and Cambodia). Taken together, all these resources are designed to meet the peak demand of 1,068 MW (EDC, 2016).

2.2 Data

Different datasets were obtained as inputs to the reservoir and power system models. Inputs to reservoir system model include reservoir specifications (Table 1) and time series of observed inflow and inflow forecasts. Since long and reliable time series of observed river discharge are not available, we retrieved inflow data for the six reservoirs from the

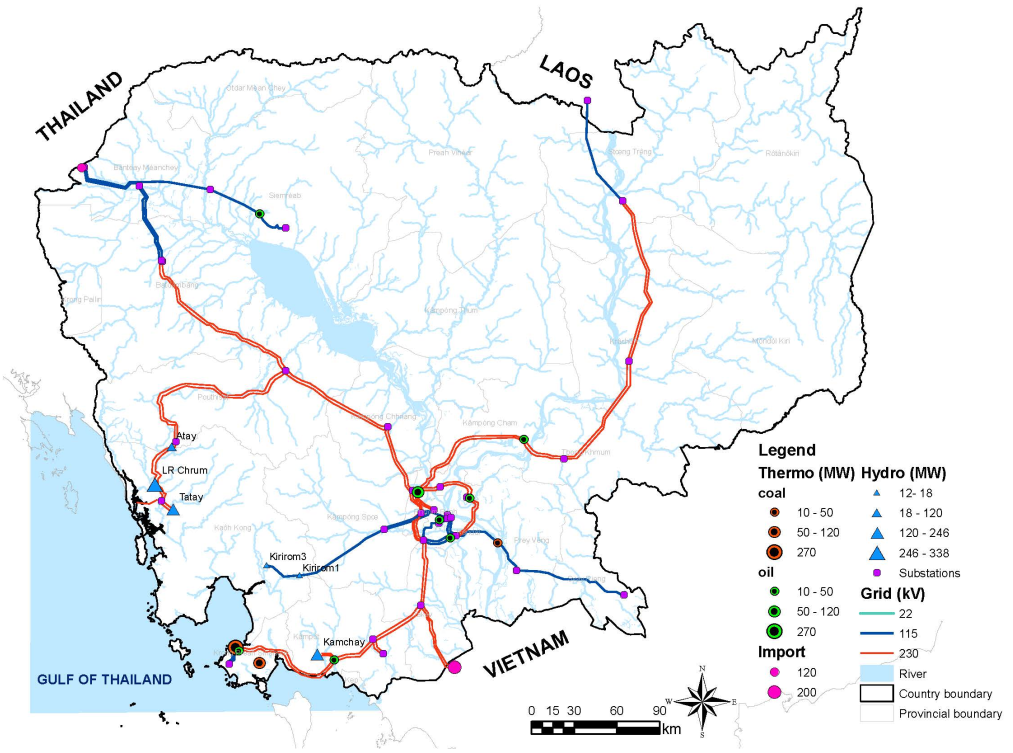

Figure 1. Main components of the Cambodian water-energy system, as of 2016. The circles represent the thermoelectric plants (coal and oil) and imports from neighbouring countries, while the triangles represent the hydropower plants. The purple squares and segments denote the substations and transmission lines, respectively. The river network is shown in light blue. Further details are provided in Section 2.1

.

Table 1. Design specifications of the Cambodian hydropower dams (EDC, 2016).

Name	Installed capacity (MW)	Dam height (m)	Storage (Mm^3)	Design discharge (m^3/s)	Hydraulic head (m)	Basin area (km^2)
Kamchay	194.1	110	680	163.5	122	710
Kirirom I	12	34	30	20	373.5	99
Kirirom III	18	40	30	40	271	105
Atay	240	45	443.8	125	216	1,157
LR Chrum	338	68	62	300	132	1,550
Tatay	246	77	322	150	188	1,073

Global Flood Awareness System (GloFAS) (Harrigan et al., 2021), a data source that (i) is commonly used in developing Asian countries (MacLeod et al., 2021) and (ii) allows us to model the water-energy system with a reasonable degree of accuracy (Koh et al., 2022). For consistency, we adopted the streamflow forecasts issued by GloFAS, which consists of an 11-member ensemble (Zsoter et al., 2020). The inflow data are available from 1979 to near real-time with daily resolution. Inflow forecasts are available for two days weekly (every Monday and Thursday) with a 24-hour time step and up to 46-day lead time. Forecasts are available from January 1999 to December 2018. The common period (2000-2018) was selected for all experiments.

For the power system model, required data include the specifications of the transmission lines and generators, as well as hourly time series of electricity demand at each substation. The line and generator details were extracted from technical reports (EDC, 2016; JICA, 2014), while the monthly peak demand was retrieved from the same reports. Based on the available monthly peak demand and hourly demand profiles for weekdays and weekends, we distribute the national demand to each substation on the basis of its voltage level. The detailed methodology for deriving the electricity demand time series is reported in Koh et al. (2022).

3 Modelling framework

3.1 Overview

As illustrated in Figure 2, the components of our computational framework are (1) a reservoir system model, (2) a power system model, and (3) a reservoir re-operation model. Note that the 'typical' representations of water-energy models include only the first two components: the reservoir model releases water according to its operating rules, and the amount of available hydropower is communicated to the power system model, which then dispatches (part of) the available hydropower depending on the specific dynamics of the power grid. This approach of separately modelling the water and power systems with a one-way information flow is known as 'soft-coupling' (Voisin et al., 2006; Chowdhury, Kern, et al., 2020; Kern et al., 2020). In our framework, we also use a reservoir re-operation model that explicitly accounts for the feedback from the power to the water system. In particular, the re-operation model gathers information on the amount of hydropower dispatched into the grid and calculates the corresponding amount of water that should be released from the dams (more details in Section 3.4). By engaging this component, the reservoir and power system models are 'hard-coupled', thus representing a situation in which the reservoir operations are contingent upon the state of the power system (Ibanez et al., 2014; Gebretsadik et al., 2016; Koh et al., 2022).

In our study, we evaluate the value of streamflow forecasts in the Cambodian grid by first operating the system with the soft-coupling approach. Doing so has two advantages. First, the unidirectional information flow provides insights into how the value of streamflow forecasts changes as we move from performance metrics focussing on the reservoir system to metrics focussing on the power system. Second, the lack of a tight operational integration between the two systems yields a larger operating space, allowing us to identify stressors (e.g., forecast skill) that control system performance—and that could be 'masked' by the presence of the feedback between the energy and water system. In the second part of our experiments, we incorporate the feedback mechanism between the systems by introducing the reservoir re-operation model. This adds one more stage to the modelling process, where the amount of hydropower dispatched by the power system is communicated back to the reservoir system model. Doing so provides insights into how the role played by streamflow forecasts within the power grid changes when the operating space is reduced.

3.2 Reservoir system model

The daily amount of hydropower available at each reservoir is determined by the reservoir system model through its release decisions, which can be determined by two alternative schemes: (i) a benchmark one based on static rule curves, and (ii) a more complex scheme that dynamically integrates the streamflow forecasts.

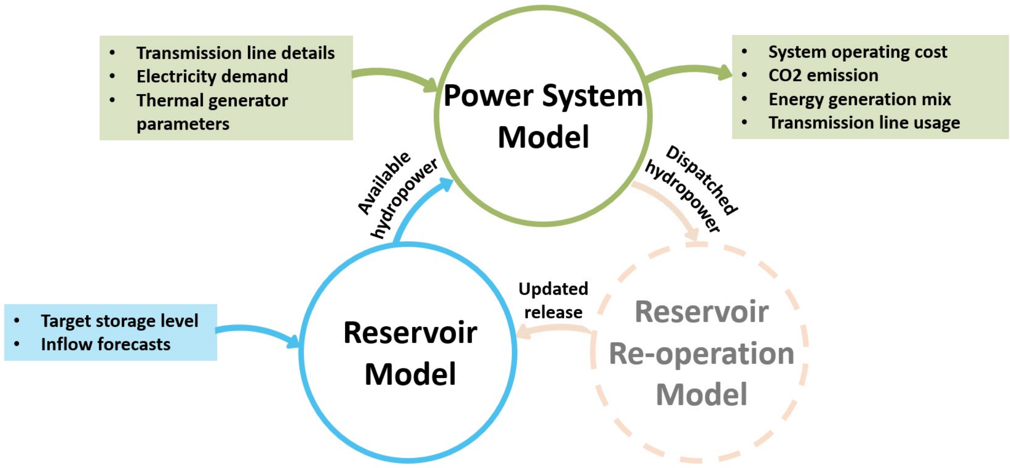

Figure 2. Schematic of the computational framework, comprising a reservoir system model, a power system model, and a reservoir re-operation model. The arrows represent the information flow between modelling components. The circles for the reservoir and power system models are in solid lines to represent the fact that these components are 'typically' considered in water-energy studies, where a water model provides the boundary conditions for a power system model. The dashed circle around the re-operation model indicates that this is an optional model that can be engaged when needed.

3.2.1 Benchmark scheme: rule curves

The storage dynamics of the i-th reservoir are described by the following mass balance, solved with a daily time step:

$$\begin{aligned} S_d^i = S_{d-1}^i + Q_d^i - R_d^i - spill_d^i - E_d^i, \\ 0 \leq S_d^i \leq S_{cap}^i, \\ Q_{MEF,d}^i \leq R_d^i \leq R_{max}^i, \end{aligned} \tag{1}$$

where S_d^i is the reservoir storage on day d, Q_d^i the reservoir inflow (between day $d-1$ and d), R_d^i the volume of water released through the turbines, $spill_d^i$ the volume of water spilled from the reservoir, E_d^i the evaporation losses from the dam, and S_{cap}^i the capacity of the dam.

An example of the rule curves we adopted is illustrated in Figure S1 (in the SI). Each rule curve is composed of a piecewise linear function based on the maximum and minimum water levels that the reservoir should reach within a calendar year (H_1^i and H_2^i) and the time of year in which these values should be reached (T_1^i and T_2^i). The concept of defining reservoir operating rule curves in this manner was proposed by Oliveira and Loucks (1997) and subsequently adapted in several other studies (e.g., Liu et al. (2011); Yassin et al. (2019)). Its use in representing actual system operations in Southeast Asia has also been validated (Chowdhury, Kern, et al., 2020; Dang et al., 2020). As an offline operating policy, the daily release decision R_d^i is made to bring the actual storage as close to the target storage as possible, while being subjected to an upper bound (R_{max}^i) and lower bound ($Q_{MEF,d}^i$). R_{max}^i is the maximum volume of water that can be turbined (representing the designed discharge capacity of the dam), while $Q_{MEF,d}^i$ represents the downstream environmental flow requirement, calculated according to the method used in Pastor et al. (2014).

Finally, the daily available hydropower for the i-th reservoir is calculated as follows:

$$HP^i_d = \eta \times \rho \times g \times R^i_d \times (H^i_{d-1} + H^i_d)/2, \tag{2}$$

where HP^i_d is the available hydropower (MW) on day d, η the turbine efficiency, ρ the water density (1000 kg/m^3), g the gravitational acceleration (9.81 m/s^2), and H^i_d the hydraulic head, taken as the average between days $d-1$ and d. For dams operated in cascade, Eq. (1) is updated to account for the natural inflow as well as the turbined and spilled water from the upper reservoir(s).

3.2.2 Forecast-informed scheme

In contrast to the benchmark scheme—where the reservoir release is only contingent upon the target water level—operating with streamflow forecasts allows the operators to make release decisions based on the knowledge available for the future inflows. In turn, this allows the system to prepare for impending wet or dry events. To integrate this information, the reservoir operation scheme employs a deterministic Model Predictive Control (MPC) approach (Galelli, Goedbloed, et al., 2014; Turner et al., 2017; Lee et al., 2022). According to this scheme, at the beginning of day d, the model receives a deterministic streamflow forecast for the next H days for each reservoir i ($Q^{f,i}_d, \ldots, Q^{f,i}_{d+H-1}$), and optimizes the release over that finite horizon (i.e., days $[d, d+H-1]$) according to a pre-defined objective function. In our work, consistent with the operating rules, we seek to explicitly maximize the hydropower generated by each dam. To prevent an over-aggressive release profile, we impose a penalty on the final state of the reservoir storage at the end of the forecast horizon (Soncini-Sessa et al., 2007), ensuring that it does not deviate too much from the target water levels (Figure S1). This yields the following optimization problem for each reservoir i:

$$\max_{R^i_d, R^i_{d+1}, \ldots, R^i_{d+H-1}} \sum_{t=d}^{d+H-1} HP^i_t - X(s^i_{t=d+H-1}), \tag{3}$$

where HP^i_t is the amount of hydropower produced by the i-th reservoir in one day and $X(\cdot)$ is the penalty associated to the storage on day $(d+H-1)$. HP^i_t is derived from Eq. (2) as a result of iteratively solving, over H days, Eq. (1) with Q^i_d replaced by the streamflow forecast $Q^{f,i}_d$. The release decisions are thus bounded by $Q^i_{MEF,d}$ and R^i_{max}. The output of the optimization problem (block of H days) is a time series of release decisions $R^i_d, R^i_{d+1}, \ldots, R^i_{d+H-1}$. Contingent upon the actual inflow (Q^i_d), we implement the release for the first day (R^i_d), and calculate the mass balance for each reservoir according to Eq. (1). The actual hydropower produced (HP^i_d) derived through Eq. (2) is then communicated to the power system model for dispatch. In sum, prior to each day d, we solve multiple MPC problems (one for each hydropower reservoir) with the aim of maximizing the hydropower generation for each reservoir over the next H days, yielding a sequence of reservoir releases as decision variables ($R^i_d, R^i_{d+1}, \ldots, R^i_{d+H-1}$).

3.3 Power system model

The power system model is PowNet, a production cost model that solves a mixed integer linear program with the objective of fulfilling the hourly electricity demand at minimum cost (Chowdhury, Kern, et al., 2020). The decisions made by PowNet include, for the next 24 hours, (i) which generating units to start-up and shut down (unit commitment) and (ii) the amount of power supplied by each unit (economic dispatch). Key inputs to PowNet include transmission line parameters, hourly time series of electricity demand at each sub-station, techno-economic parameters of thermoelectric generators (e.g., capacity, operations and maintenance costs), and the hydropower available at each dam calculated by the reservoir system model (Section 3.2). In scheduling the hourly production, the model is subject to multiple constraints, including ramping limits, generation limits, minimum up and down-time of each generator, and transmission capacity constraints. The decision variables at each hour thus include binary variables (e.g., generating unit to use and whether to switch it on or off) and continuous ones (e.g., electricity generated by each unit, voltage angle at each node, spinning and non-spinning reserves, amount of renewables and imports dispatched). For each simulated day, PowNet outputs include hourly time series of operating costs, CO_2 emissions, generation mix, and transmission line usage. PowNet has been applied to multiple national grids, such as the ones of Cambodia (Chowdhury, Kern, et al., 2020), Laos (Chowdhury, Dang, et al., 2020), and Thailand (Chowdhury et al., 2021; Galelli et al., 2022).

3.4 Reservoir re-operation model

The reservoir re-operation model is introduced as a means to capture the feedback between interdependent water-energy systems. Serving as a bridge between the reservoir and power system, this model compares the amount of available hydropower produced by the i-th reservoir (HP_d^i) with the amount dispatched by the power system (HP_d^{i*}). With the goal of reducing the mismatch between these two values, the re-operation is triggered when there is an over-production of hydropower (i.e., $HP_d^{i*} < HP_d^i$). The re-operation algorithm (refer to Koh et al. (2022) for details) then re-calculates the reservoir release such that the i-th reservoir releases only the amount R_d^{i*} ($< R_d^i$) needed to produce HP_d^{i*}. In this study, all reservoirs are re-operated in the scenario where the feedback between the systems is considered. Operating in this manner offers flexibility whereby the release decisions made by the hydropower reservoir can be updated based on real-time information regarding the power system. In other words, this allows each reservoir to be used as a ‘battery’, so water can be stored for future use. Doing so may alter the value of forecasts, as the operations of the reservoirs would then depend on the state of the power system as well.

4 Experimental setup

The goal of our study is to quantify the value of streamflow forecasts for power system operations, understand how the value changes with skill, and determine when the value matters the most. We use multiple benchmarks to characterize system operations under different conditions and thus meet our goals. First, we use the benchmark scheme (Section 3.2.1), i.e., static rule curves, to characterize reservoir operations. Subsequently, we compare the results to the forecast-informed scheme. Here, we introduce two benchmarks, perfect forecasts and climatology, both commonly used to assess the value of streamflow forecasts (Grantz et al., 2005; Zhao et al., 2012; Yossef et al., 2013; Zimmerman et al., 2016; Nayak et al., 2018; Anghileri et al., 2019; McInerney et al., 2020; Quedi & Fan, 2020). To characterize the skill-value relationships, we have at our disposal multiple forecasts within the ensemble, so one could perform weighted aggregation on the members or consider each member as a separate deterministic forecast (Slater et al., 2016; Delaney et al., 2020). We consider both, that is, (i) we take the ensemble mean across the 11 members (more details in Section 2.2), and (ii) we use the individual members as independent inputs. In sum, we run our simulations under 14 different forecast scenarios—i.e., perfect forecasts, climatology (taken as a 365-calendar day average from the inflow data), ensemble mean, and each of the 11 members. Taking into account how system operations may depend on the state of the power system as well, we repeat the experiments with the feedback from the power system back to the reservoir model. This means that our experiments are conducted (i) with 14 different deterministic forecast scenarios, and (ii) without and with feedback.

The forecast horizon selected in our study is 30 days based on the power generation mix obtained by preliminarily testing the system operations with different forecast horizons (see Table S1 in the SI for additional details). Since the reservoirs in our model are operated at the daily time step while the forecasts are only available on every Monday and Thursday of each week (Zsoter et al., 2020), we fill the gaps (Tuesday-Wednesday, Friday-Sunday) by extracting a 30-day window from the 46-day availability, and shifting the forecast one-day ahead, until the next set of forecasts is available. For example, the forecast for a given

Monday would be from day 1 to day 30 (out of the available 46 days), and the forecast for Tuesday would be from day 2 to 31 for the same set of 46 days. This is repeated for Wednesday; on Thursday, a new set of forecast is available again. Based on simulations ran on an Intel(R) Core (TM) i7-8700 CPU 3.2 GHz with 8 GB RAM running Windows 10, the runtime is approximately 20 hours for each simulation. The total runtime for 14 scenarios is thus approximately 280 hours. The experiments including the feedback from the power to the water system are more computationally demanding, taking about 40 hours each to complete.

Moving to the specific metrics that can be used to quantify forecast skill for deterministic forecasts, it is worth stressing that the options are many (Huang & Zhao, 2022). In this study, we considered the use of the Nash-Sutcliffe efficiency (NSE) (Nash & Sutcliffe, 1970), Pearson correlation coefficient (Lima & Lall, 2010; Li et al., 2014) and Symmetric Mean Absolute Percentage Error (SMAPE) (Ogliari et al., 2021). Since the forecast skill is calculated for each reservoir within the system, a spatial aggregation is necessary to represent the overall skill for the entire study area and contrast it against performance metrics defining forecast value (e.g., CO_2 emissions). The primary criterion for the chosen metric is that it has to be bounded to prevent skewed values upon aggregation, thus eliminating NSE $(-\infty, 1]$ as a candidate. As for the Pearson correlation coefficient, there is a possibility of positive and negative values cancelling each other out during the aggregation process, thus misleading both the strength and direction of the relationship between the actual and forecast time series. SMAPE is an accuracy metric that measures the difference between the actual and forecast data between 0 and 1, and is a metric that fulfills both requirements for our study. All candidate metrics are illustrated in Figure S2; across the reservoirs, forecast errors tend to be larger during the pre-monsoon (Feb-Apr). The skill then progressively increases until the end of the year. To derive the overall skill of a forecast member across space, we perform a weighted average of the errors with respect to the hydropower plant capacities following Eq. (4):

$$SMAPE_d = \sum_{i=1}^{N} (w_i * SMAPE_{i,d}), \tag{4}$$

where $SMAPE_d$ is the aggregated forecast error on day d, w_i is the weight of the i-th reservoir, taken as the hydropower capacity divided by the total capacity of the N reservoirs, and $SMAPE_{i,d}$ is the forecast error for the i-th reservoir on day d.

As for the forecast value, we consider six metrics: the available, dispatched, and unused hydropower, system operating costs, CO_2 emissions, and the number of N-1 violations—i.e., instances in which any of the high-voltage lines reaches 75% of its capacity—an indicator of grid stress. Here, note that the available hydropower is an output of the reservoir system model (derived through Eq. (2)), a commonly-used metric to assess forecast value in previous studies (Lee et al., 2022; Anghileri et al., 2019). The other metrics are produced by the power system model, and are thus chosen to represent multiple performance aspects of the grid. First, the hydropower metrics provide insights into how forecast value is transferred from the water system to the power system. Next, the system operating costs and CO_2 emissions provide insights into how system operations are impacted by different levels of forecast accuracy. Last, the N-1 violations indicate how stressed the transmission lines are. This is important, since (i) grid stress is considered one of the triggers for blackouts (Veloza & Santamaria, 2016), and (ii) can serve as an indicator of system performance (e.g., when line capacity limits the penetration of renewables in the grid (Chowdhury, Dang, et al., 2020)). In assessing the skill-value relationship, we note that there are other input variables (from both the reservoir and power system) that may influence the overall system performance. As such, besides forecast skill, the actual inflow (Q) and the electricity demand are also considered as system stressors.

5 Results

In this section, we first evaluate the benefits that lie in adopting streamflow forecasts when operating hydro-dominated power systems (Section 5.1). This is done by comparing results obtained from simulating the reservoir and power systems under different benchmark operating schemes. Then, we investigate how the value of forecasts changes with skill (Section 5.2). Here, we investigate the skill-value relationship under both standard operations (i.e., without feedback; Section 5.2.1) and operations with feedback between the power and water systems (Section 5.2.2). Such comparison illustrates how the value changes as we capture the interdependencies between water and power systems.

5.1 Value of streamflow forecasts

5.1.1 Comparison across multiple performance metrics

To determine the value of streamflow forecasts in power system operations, we aggregate the five key performance metrics across both space and time (since the reservoir model is run with a daily time-step and the power system model with an hourly time-step). The metrics include system-wide available and dispatched hydropower, system operating costs, CO_2 emissions, and number of N-1 violations (Figure 3). For comparison, we include the results for operations guided by rule curves and three different forecast-informed schemes, namely perfect forecasts, climatology, and the ensemble mean. At the monthly timescale, a strong seasonal pattern can be observed across all metrics. Despite the similar pattern exhibited by the different operating schemes, it is clear that the use of streamflow forecasts affects the operations of both reservoir and power system.

5.1.1.1 Available hydropower. Temporally, the system behavior can be classified into three periods, namely pre-monsoon (Feb-Apr), summer monsoon (May-Oct), and post-monsoon (Nov-Jan). The value of streamflow forecasts largely varies across these periods. We first focus on the amount of available hydropower, a direct product of the reservoir system model (boxplot in the top panel of Figure 3). Across all scenarios, the hydropower availability increases from the pre-monsoon to peak at the end of the monsoon, before decreasing again. This follows the seasonal pattern of the summer monsoon, a key feature of Southeast Asian climates (Chowdhury et al., 2021). Operating the reservoirs using rule curves results in larger hydropower availability than the schemes with forecasts during the pre-monsoon and monsoon period (see the corresponding mean and standard deviation in Table 2). During the monsoon, operating the dams without streamflow forecasts generates an average of at least 40 GWh more hydropower each month than the other schemes. This result is attributed to the nature of the decisions made with rule curves: without forecast, the release decisions of each reservoir are made with respect to the target storage only. As such, the reservoirs tend to release water whenever they receive large inflow volumes, resulting in large hydropower availability. Consequently, after the monsoon, the reduced inflow also causes the reservoirs to make smaller releases. The hydropower availability thus drops significantly (by 40–60% from November to December), averaging at least 60 GWh/month less than the forecast-informed schemes. In other words, this sharp decline is due to the myopic nature of the rule curves. In contrast, operating with forecasts allows the reservoirs to maintain a larger hydropower production after the monsoon. Looking at the specific forecast-informed schemes, we observe that operating with perfect foresight produces the best results throughout all seasons—a result that is consistent with past studies (Anghileri et al., 2019; Ahmad & Hossain, 2020; Doering et al., 2021; Guo et al., 2021; Lee et al., 2022).

5.1.1.2 Power-related metrics. The circles in the top panel of Figure 3 represent the hydropower dispatched within the grid. The first point to make is that not all available hydropower is dispatched by the grid. The mismatch between available and dispatched hydropower is accentuated during the monsoon season, when the amount of dispatched hy-

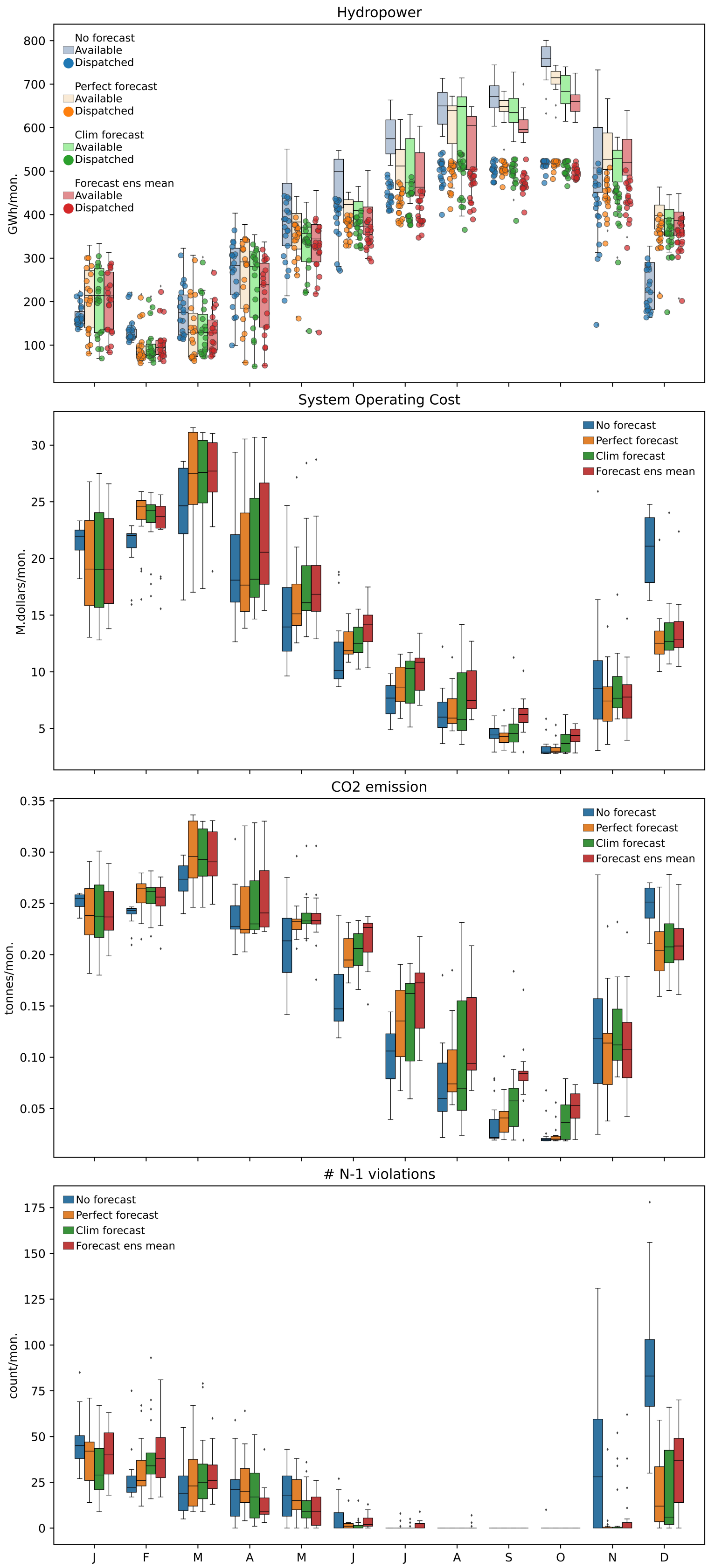

Figure 3. Monthly variability in system performance under different forecast-informed schemes. The four panels illustrate the range of variability in hydropower (available and dispatched), system operating costs, CO_2 emissions, and frequency of N-1 violations, respectively. All variables are spatially aggregated across the entire power system. Within each panel, the results from three forecast-informed schemes (perfect forecasts, climatology, and ensemble mean) are compared to the benchmark (no forecasts). Experiments are conducted without feedback between the reservoir and power systems.

Table 2. Variability in mean and standard deviation of the performance metrics illustrated in Figure 3 across different operating schemes (no forecasts, perfect forecasts, climatology and ensemble mean) and periods (pre-monsoon, monsoon and post-monsoon).

Performance metric	Scenario	Pre-monsoon	monsoon	Post-monsoon
Available hydropower (GWh/mon.)	No forecasts	195.16± 83.11	584.51±137.29	302.19±173.18
	Perfect forecasts	164.98±101.99	539.87±136.00	377.93±151.97
	Climatology	159.95± 91.11	527.80±142.82	360.75±142.47
	Ensemble mean	151.60± 78.62	506.85±132.20	366.82±146.94
Dispatched hydropower (GWh/mon.)	No forecasts	191.04± 76.31	451.26±71.55	267.27±120.78
	Perfect forecasts	160.62±94.75	439.50±76.23	329.83±114.60
	Climatology	157.17±86.50	431.12±82.74	319.20±111.61
	Ensemble mean	149.58±75.94	415.42±77.53	323.97±113.65
Unused hydropower (GWh/mon.)	No forecasts	4.12± 8.12	133.26± 69.40	34.92± 55.00
	Perfect forecasts	4.36± 8.57	100.37± 62.29	48.10± 40.90
	Climatology	2.78± 5.62	96.68± 62.58	41.54± 33.51
	Ensemble mean	2.02± 3.65	91.42± 56.61	42.85± 36.16
System operating cost (M.dollars/mon.)	No forecasts	21.58± 4.13	8.02± 4.70	17.28± 6.65
	Perfect forecasts	23.47± 5.21	8.67± 4.99	13.34± 5.91
	Climatology	23.68± 4.81	9.17± 5.39	13.99± 5.79
	Ensemble mean	24.16± 4.42	10.11± 5.12	13.70± 5.87
CO_2 emission (tonnes/mon.)	No forecasts	0.25± 0.02	0.10± 0.07	0.21± 0.07
	Perfect forecasts	0.27± 0.04	0.12± 0.08	0.18± 0.07
	Climatology	0.27± 0.03	0.13± 0.08	0.19± 0.06
	Ensemble mean	0.27± 0.03	0.14± 0.07	0.19± 0.07
# N-1 violations (hours/mon.)	No forecasts	22.96± 15.00	3.98± 9.32	59.16± 40.45
	Perfect forecasts	27.70± 15.67	3.39± 7.78	20.07± 21.10
	Climatology	30.00± 19.83	2.42± 6.13	20.65± 21.05
	Ensemble mean	27.63± 17.32	2.76± 5.42	26.21± 22.36

dropower not does not increase with hydropower availability. In fact, its value stabilizes around 450 GWh/month, leading to a larger discrepancy between the two metrics. This indicates a condition of over-production, a situation in which the grid is unable to dispatch all the available hydropower due to oversupply or limited transmission capacity. The percentage of total dispatched hydropower with respect to the total available for the four scenarios (no forecasts, perfect forecasts, climatology, and ensemble mean) over 19 years is 81.7%, 84.4%, 84.9%, and 85.1%, respectively. The discrepancy peaks at the end of the monsoon season, with up to 35%, 29%, 29%, and 28% of hydropower unused in the four scenarios, respectively. This indicates that defining value in terms of different performance metrics can produce varying conclusions. The current practice of defining value in terms of available hydropower (determined by a water system model), may therefore overlook the disparity between the available and dispatched hydropower, especially during the monsoon. To achieve a comprehensive understanding of streamflow forecast values, it is therefore important to evaluate the responses of multiple performance metrics spanning across water and power systems.

With the largest installed capacity in the grid (about 50%), hydropower fulfills more than half of the overall electricity demand in Cambodia. The amount of hydropower within the system thus plays a paramount role in determining the power system operations and the energy generation mix (refer to Figure S3 in the SI), which directly affects operating costs and CO_2 emissions. Referring to the second and third panel in Figure 3, an observation similar to the case of hydropower can be made; the benefits of operating with forecasts are accentuated during the post-monsoon season. Towards the end of the monsoon (in October), the scheme with perfect forecasts outperforms all other scenarios in terms of operating costs, and is comparable to the case without forecasts in terms of CO_2 emissions. This suggests that while the use of forecasts may not be very beneficial to the system during the pre-monsoon and the peak of the monsoon, given the right conditions, a better forecast can be advantageous from an earlier point in time to achieve lower operating costs and CO_2 emissions. A larger amount of hydropower in the grid also reduces stress in the transmission line, a point illustrated by the frequency of N-1 violations. There are, in particular, three transmission lines that are periodically stressed, two of which are part of a network that feeds Phnom Penh, Cambodia's capital and main load-centre (see Figure 1). The line congestions are eased as less pressure is placed on the thermal plants to fulfil the high demand. After the monsoon, the scenarios with forecasts are able to sustain the hydropower production, allowing more hydropower to be dispatched in the grid as opposed to the scenario without forecasts.

Given these results, it is evident that the use of streamflow forecasts is valuable to power system operations in terms of (i) reducing hydropower over-production during the monsoon, (ii) maintaining hydropower supply after the monsoon, and (iii) reducing transmission line stress. Importantly, these points are revealed by the use of a modelling framework accounting for both water and power system dynamics, something that would be hidden if one were to use a reservoir system model, thereby only focussing on the available hydropower. This highlights the complexity of the coupled water-energy system and the importance of exploring the multiple roles played by forecasts as we move beyond a water reservoir system.

5.1.2 Intra- and inter-annual variability of forecast value

Better understanding the inter- and intra-annual variability of forecast value can provide a deeper insight into when and why forecasts matter to grid operations in hydro-dominated power systems. To support this analysis, we focus solely on dispatched hydropower (which largely affects the power generation mix), and introduce a metric defined as the difference between the hydropower dispatched by each forecast-informed scheme and the one dispatched when adopting rule curves. Hence, positive values mean that a forecast-informed scheme performs better than rule curves. The values illustrated in Figure 4 reveal a few interesting insights. First, the benefit associated to forecasts is most of the time negative between February and October, meaning that forecasts are in general not beneficial during the pre-monsoon and monsoon seasons. This is in contrast to the period between November and January (post-monsoon season), when positive benefits are observed. Second, positive benefits extend to almost 200 GWh/month, while the negative ones to less than -100 GWh/month. This indicates that the extent of benefits derived from using forecast-informed schemes, albeit less frequent, is more significant. Third, there are a few instances in which positive benefits are observed during the the pre-monsoon and monsoon seasons (e.g., April 2007, June 2010, July 2004). These episodes are due to specific, and unexpected, fluctuations in dam inflow for that particular year. In 2007, for instance, the 30-day outlook shows that the inflow will keep increasing in May, therefore the reservoirs release more water and produce more hydropower, which is then dispatched into the grid (refer to Figure S4 in the SI). This information is unknown to the scheme without forecast, explaining the larger benefits derived in April 2007.

Looking at the inter-annual variability, our results show that the three best and worst performing years are 2000, 2001, 2018, and 2002, 2005, and 2008, respectively. A closer look at the reservoir inflow corresponding to each year, shown in Figure 5, gives us two insights regarding the hydrological conditions that are favorable to forecast-informed schemes. First, larger inflow volumes tend to be beneficial. Second, and perhaps more interesting, forecasts are more useful when the inflow patterns present sudden and unexpected changes; a situation that can be hardly managed when controlling a reservoir system with rule curves.

5.2 Skill-value relationship

To understand how forecast value changes with skill, we conducted deterministic simulations using the 11 individual streamflow forecast members. We then investigate the skill-value relationship under two reservoir operating schemes: (i) without (Section 5.2.1) and (ii) with (Section 5.2.2) feedback between the reservoir and power systems. This allows us to characterize the skill-value relationship under different levels of integration of the coupled water-energy system.

5.2.1 System operations without feedback

To study the relationship between forecast skill and value, we define skill using the forecast error (Section 4) and relate it to difference performance metrics that characterize forecast value, namely available, dispatched, and unused hydropower, system operating costs, CO_2 emissions, and number of N-1 violations. In our analysis, we also consider two additional variables, or stressors, that may affect system performance. These are the inflow to the reservoirs and electricity demand, or load. All these variables are then analyzed through a correlation matrix and a multiple linear regression model, whose results are reported Figure 6.

Beginning with the correlation analysis (left panel), our results show that the correlation between stressors and performance is significant ($p < 0.05$) for most stressor-metric pairs. Beginning with the forecast error, we note two important patterns. First, there is a strong negative correlation between error and available and dispatched hydropower, meaning that, as the error increases, the contribution of hydropower to the generation mix decreases. In turn, this explains the positive correlation with costs, CO_2 emissions, and N-1 violations (recall that the power system must rely more on thermoelectric power and imports when less hydropower is available). Second, the strength of the relationship between forecast error and performance metrics decreases as we move from the reservoir system to the power system, a result that is explained by the fact that other stressors become relevant when studying coupled water-energy systems. Inflow, for instance, positively affects hydropower-related and negatively affects costs, CO_2 emissions, and grid stress. An increase in load, on the other hand, implies an increase in costs and CO_2 emissions.

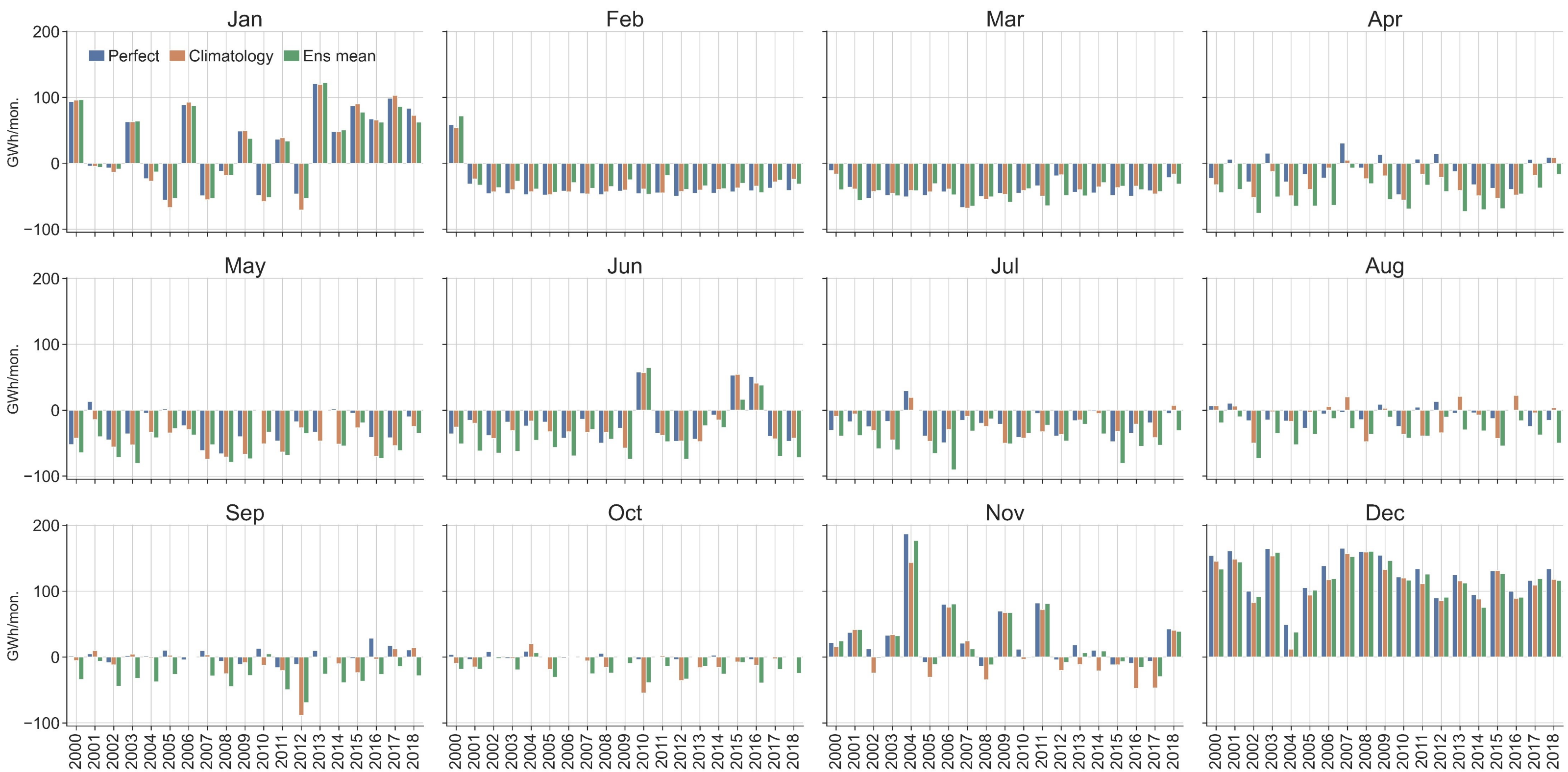

Figure 4. Benefit of using streamflow forecasts at different times of the year, defined as the difference between the amount of hydropower dispatched with and without forecast. The results are grouped according to calendar months (12 panels) and year (horizontal axis). Each cluster of three bars represents the three forecast-informed schemes: perfect forecasts, climatology, and ensemble mean. The values shown are the positive/negative benefits of using each kind of forecast, i.e., the difference between the hydropower dispatched by each forecast-informed scheme and the one dispatched when adopting rule curves.

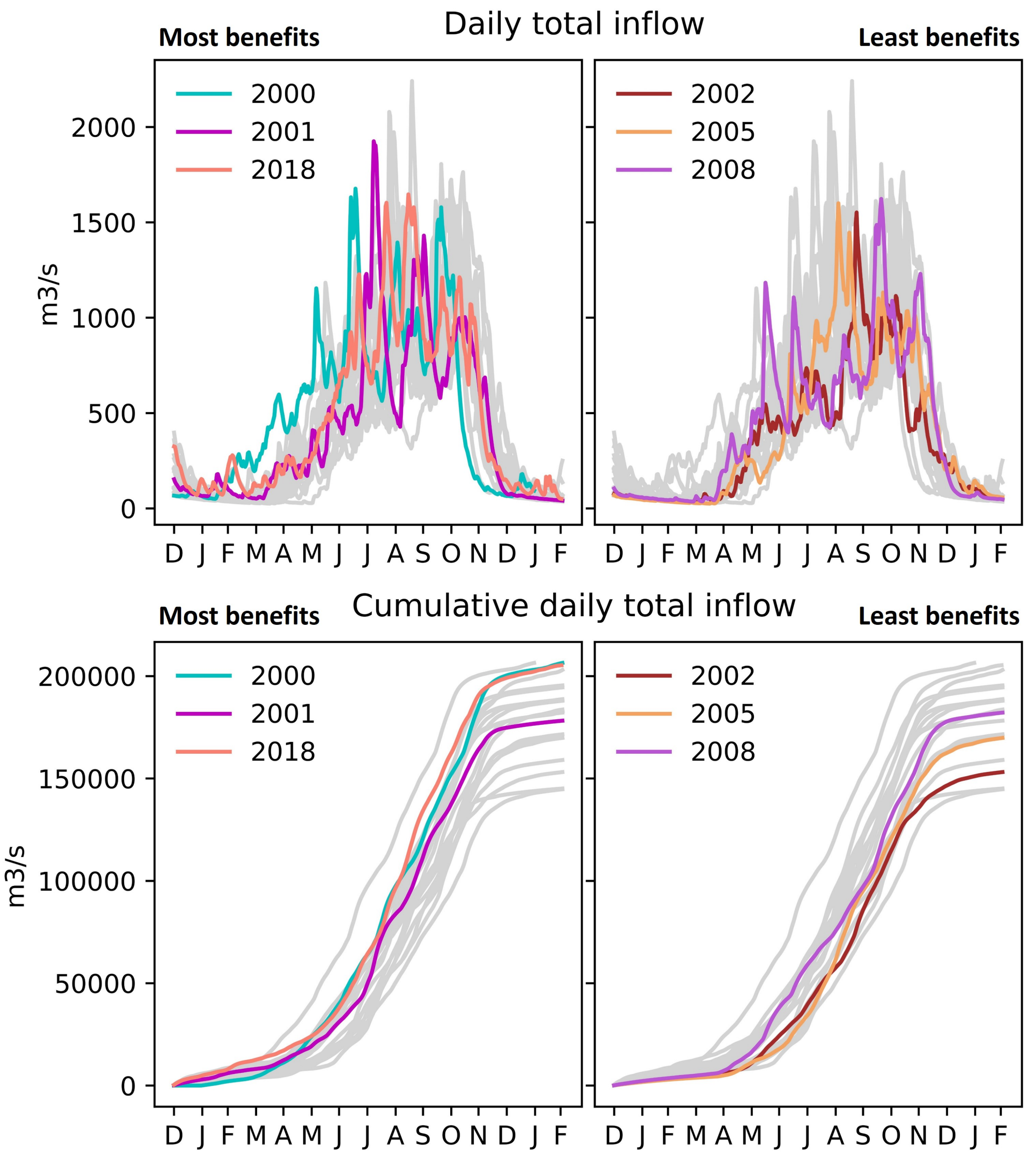

Figure 5. Comparison of daily time series (top panels) and cumulative (bottom panels) inflow profiles across different years. Each gray line represents one year between 2000 and 2018. Based on the total hydropower dispatched each year, three years with the highest and lowest benefits are identified and highlighted in the left and right panels, respectively.

To further understand how forecast error, inflow, and load control the performance metrics, we identify multiple linear regression models in which the inputs are the significant independent variables (predictors) and each of the six metrics are the dependent variables (predictands). All variables are first standardized (by subtracting the variable's mean from each observed value and then dividing by the variable's standard deviation) to facilitate the comparison. Using a forward selection approach, the predictors are iteratively added to the regression model, beginning from the one with the highest (absolute value of) correlation coefficient r (Galelli, Humphrey, et al., 2014). From the model, the coefficient of determination (r^2) and final regression coefficients allow us to infer the contribution of each predictor to the variance of the predictands, and hence the importance of the model inputs. The variables are grouped according to the calendar months before carrying out the regression. The results are illustrated in the central and right panels of Figure 6.

Similar to the previous analyses, this analysis can also be organized around three periods, i.e., pre-monsoon, monsoon and post-monsoon. The importance of the forecast error for the available hydropower is more obvious during the post-monsoon season, since a discrepancy between observed and predicted inflow determines how well the system can adapt to foreseen changes in reservoir inflow and overall transition into the dry season. This is in contrast to the monsoon season, when the reservoirs usually release close to the maximum designed release, reducing the importance of forecast errors. Moving to the next metric, the dispatched hydropower is determined through power system operations. During the pre-monsoon, less hydropower is produced, and whatever is produced usually gets fully utilized. The importance of inflow and error to hydropower usage is thus similar to that of hydropower production between February and April. During the monsoon, however, the abundant hydropower production forces the electricity demand to be the limiting factor for the amount of dispatched hydropower, explaining the importance of load during this period. Regardless of the error or inflow, the power system constraints dictate the grid usage. The dynamics between the available and dispatched hydropower also directly influence the next metric, i.e., the unused hydropower. As seen from the regression coefficients, a reduction in load can create a more than proportionate increase in the amount of unused hydro. The over-production peaks in October across all forecast-informed schemes, with about 30% unused hydro. Figure 6 also suggests that the forecast errors become insignificant beyond the first two performance metrics, since the power system performance depends primarily on inflow and load.

Breaking down the relative contributions of forecast errors, reservoir inflow, and electricity demand to different performance metrics highlights the complexity of the systems and the interdependencies between stressors. Streamflow forecasts are most valuable to improving power system performance during the post-monsoon by facilitating a smooth transition between the monsoon and post-monsoon seasons. A more accurate forecast allows resources to be exploited for continued hydropower availability for the grid to dispatch. As we move from the water system to the power system, the skill-value relationship becomes less significant, as the system responses depend more on the electricity demand.

5.2.2 System operations with feedback

The operations of the reservoir and power systems may not be entirely independent. To characterize the skill-value relationship under a tighter integration of the two systems, we repeat all experiments with the same inputs, but this time adding the feedback between the power and reservoir systems. This set of experiments thus makes use of the re-operation module described in Section 3.4. Using the same methodology described in Section 5.2.1, we study the relationship between the system stressors and performance metrics illustrated in Figure 7.

With the re-operation mechanism in place, the role played by electricity demand is amplified, while the importance of forecast skill (error) and reservoir inflow is largely reduced.

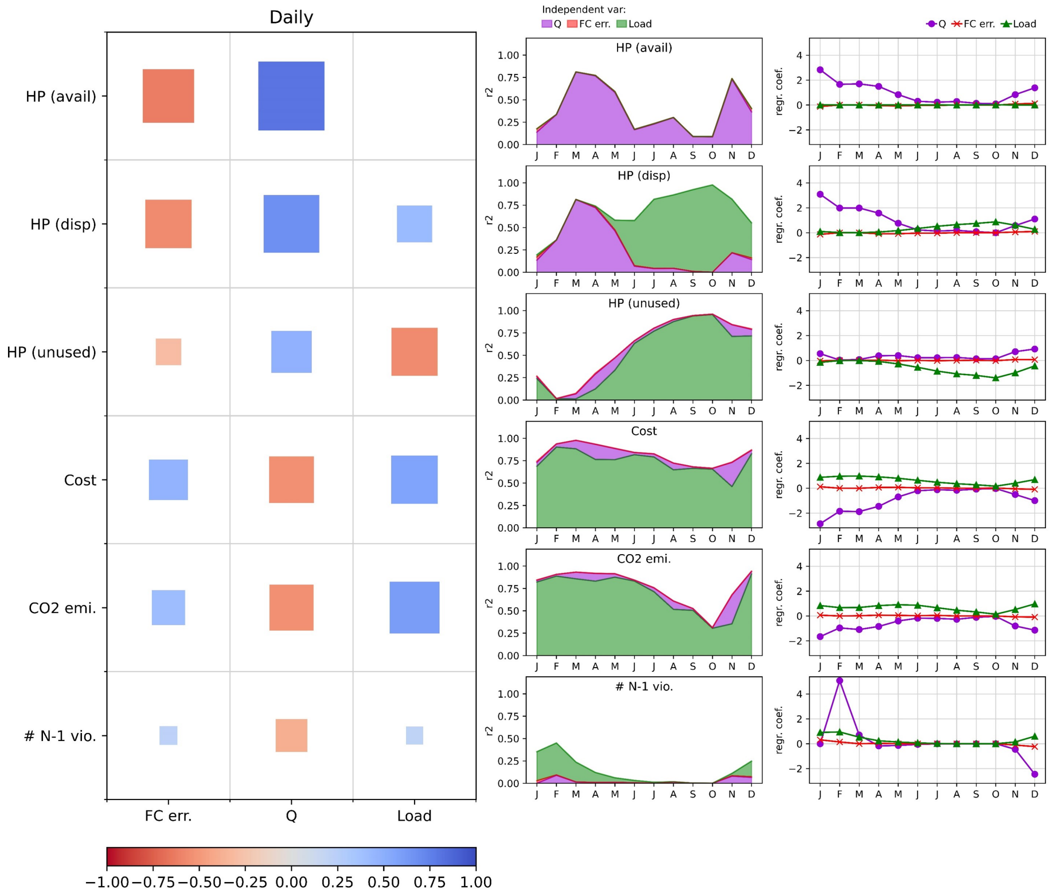

Figure 6. Relationship between system stressors (forecast error, inflow, and load) and performance metrics (available, dispatched, and unused hydropower, system operating costs, CO_2 emissions, and number of N-1 violations) illustrated by a correlation matrix (left) and regression model results (center and right). In the correlation matrix, the values (shown in the color bar) between each stressor-metric pair are obtained by bootstrapping the data through 1,000 iterations. Based on the correlation values, we first identify a multiple linear regression model between the stressors (predictors) and metrics (predictands), and then estimate the contribution of each predictor to the explained variance (center) and the corresponding regression coefficients (right). These results are reported for the scenarios that do not include the feedback between the power and water system.

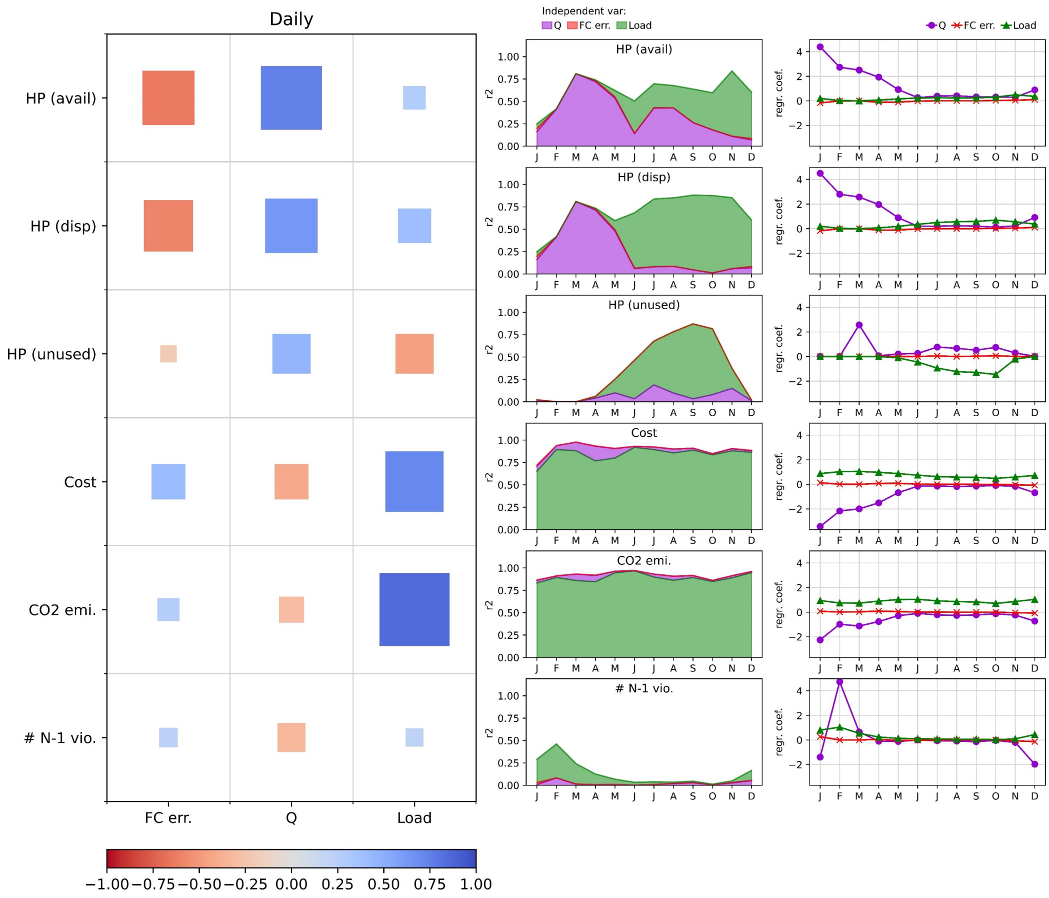

Figure 7. Relationship between system stressors (forecast error, inflow, and load) and performance metrics (available, dispatched, and unused hydropower, system operating costs, CO_2 emissions, and number of N-1 violations). These results are reported for the scenarios that include the feedback between the power and water system.

As the goal of the re-operation mechanism is to flexibly store and release water to generate hydropower that better matches the power system demand, the reservoir storage patterns can largely deviate from the seasonal patterns (Koh et al., 2022). In turn, this partially dampens the impact of hydrological variability on power system performance, making both inflow and forecast skill less important. With hydropower-related metrics being explained by load, it follows that operating costs and CO_2 emissions can almost entirely be determined by load as well, with r^2 values close to one for every month. Evidently, the presence of the feedback mechanism reduces the value of forecasts, allowing load to dominate the operating decisions in both the reservoirs and power system.

6 Discussion and conclusions

Our study evaluates the value of streamflow forecasts in hydro-dominated power systems. The performance metrics were selected from both the reservoir and power systems to represent the hydropower generation by the reservoirs, hydropower usage within the grid, as well as economic, environmental, and reliability aspects of the power system. We show that defining forecast value in terms of different performance metrics can produce different outcomes. For instance, while previous studies often associate favorable forecasts with greater hydropower availability, we found that larger hydropower availability does not necessarily translate into more usage within the grid. Unless the excess water release can serve a second purpose—such as for groundwater storage (Nayak et al., 2018) or inter-basin transfer (Li et al., 2014)—measuring value only in terms of the available hydropower may thus overlook other important aspects, such as production costs or CO_2 emissions. Therefore, when we study hydropower systems, we should consider the role that hydropower reservoirs play, not only within the reservoir network, but also within the power system as well.

In hydro-dominated power systems, hydropower operations are highly influenced by the seasonality of reservoir inflow. As a result, the grid operations and performance exhibit a strong seasonal profile as well. In our case study, the system behavior can be classified into three periods—pre-monsoon, monsoon and post-monsoon. We show that the value of streamflow forecasts varies with these different periods. During the monsoon, the use of forecasts reduces hydropower over-production. In the post-monsoon season, operating with forecasts is beneficial to sustain hydropower supply. Accurate forecasts are especially useful during the three months after the end of the monsoon to facilitate the transition from wet to dry seasons. Better forecast skill, combined with large inflow conditions, can thus benefit the system in terms of larger dispatched hydropower, lowering operating costs and CO_2 emissions. Our analysis also shows that, with a tighter integration of the reservoir and power systems, the role played by electricity demand becomes dominant in determining operational decisions within both systems.

Looking forward, an important aspect warranting additional research is the impact of the uncertainty associated to streamflow forecasts, which could be 'operationalized' through the use of stochastic MPC schemes (Pianosi & Soncini-Sessa, 2009). Such control schemes would become particularly useful when dealing with streamflow forecasts spanning across longer timescales than those currently available for this region. Another relevant aspect to consider in the future is the integration of other forms of forecasts that could improve the operation of water-energy systems, such as electric load forecasts (Hong & Fan, 2016).

Overall, we believe that a better understanding of the value provided by streamflow forecasts to multi-sector infrastructures could promote and support their use. The need for better approaches to system operations is indeed necessary in a variety of contexts, from regions experiencing hydro-climatological shifts to regions, like Southeast Asia, that are expanding their water and power supply networks.

Notation

$\boldsymbol{S_d^i}$ Storage on day d of the i-th reservoir
$\boldsymbol{S_{cap}^i}$ Capacity of the i-th reservoir
$\boldsymbol{R_d^i}$ Volume of water released through the turbines of the i-th reservoir on day d
$\boldsymbol{R_{max}^i}$ Maximum volume of water that can be turbined from the i-th reservoir
$\boldsymbol{Q_d^i}$ Inflow on day d to the i-th reservoir
$\boldsymbol{Q_{MEF,d}^i}$ Downstream environmental flow requirement of the i-th reservoir on day d
$\boldsymbol{spill_d^i}$ Volume of water spilled from the i-th reservoir on day d
$\boldsymbol{E_d^i}$ Evaporation losses from the i-th reservoir on day d
$\boldsymbol{HP_d^i}$ Available hydropower on day d from the i-th reservoir
$\boldsymbol{HP_t^{i*}}$ Hydropower dispatched in hour t from the i-th reservoir
$\boldsymbol{H_d^i}$ Hydraulic head from the i-th reservoir on day d

Open Research Section

The data and Python scripts used to simulate the water-energy system in Cambodia for this research are available at Koh (2023) via `https://doi.org/10.5281/zenodo.8163034`.

The observed reservoir inflow data are available from `https://doi.org/10.24381/cds.a4fdd6b9` (Harrigan et al., 2021) and the reservoir inflow forecast data are available from `https://doi.org/10.24381/cds.2d78664e` (Zsoter et al., 2020). Power system parameters, including generator and transmission line specifications, as well as monthly electricity peak demand data are extracted from EDC (2016) and JICA (2014).

Acknowledgments

Rachel Koh is supported by the President's Graduate Fellowship from the Singapore University of Technology and Design.

References

Ahmad, S., & Hossain, F. (2020). Maximizing energy production from hydropower dams using short-term weather forecasts. *Renewable Energy*, *146*, 1560–1577.

Anghileri, D., Monhart, S., Zhou, C., Bogner, K., Castelletti, A., Burlando, P., & Zappa, M. (2019). The value of subseasonal hydrometeorological forecasts to hydropower operations: How much does preprocessing matter? *Water Resources Research*, *55*(12), 10159–10178.

Anghileri, D., Voisin, N., Castelletti, A., Pianosi, F., Nijssen, B., & Lettenmaier, D. (2016). Value of long-term streamflow forecasts to reservoir operations for water supply in snow-dominated river catchments. *Water Resources Research*, *52*(6), 4209–4225.

Chowdhury, A. K., Dang, T. D., Bagchi, A., & Galelli, S. (2020). Expected benefits of Laos' hydropower development curbed by hydroclimatic variability and limited transmission capacity: Opportunities to reform. *Journal of Water Resources Planning and Management*, *146*(10), 05020019.

Chowdhury, A. K., Dang, T. D., Nguyen, H., Koh, R., & Galelli, S. (2021). The Greater Mekong's climate-water-energy nexus: How ENSO-triggered regional droughts affect power supply and CO_2 emissions. *Earth's Future*, *9*(3).

Chowdhury, A. K., Kern, J., Dang, T. D., & Galelli, S. (2020). PowNet: A network-constrained unit commitment/economic dispatch model for large-scale power systems analysis. *Journal of Open Research Software*, *8*(1).

Dang, T. D., Vu, D. T., Chowdhury, A. K., & Galelli, S. (2020). A software package for the representation and optimization of water reservoir operations in the VIC hydrologic model. *Environmental Modelling and Software*, *126*.

Delaney, C., Hartman, R., Mendoza, J., Dettinger, M., Delle Monache, L., Jasperse, J., ... Evett, S. (2020). Forecast informed reservoir operations using ensemble streamflow predictions for a multipurpose reservoir in Northern California. *Water Resources Research*, *56*(9), e2019WR026604.

Ding, Z., Wen, X., Tan, Q., Yang, T., Fang, G., Lei, X., ... Wang, H. (2021). A forecast-driven decision-making model for long-term operation of a hydro-wind-photovoltaic hybrid system. *Applied Energy*, *291*, 116820.

Doering, K., Quinn, J., Reed, P., & Steinschneider, S. (2021). Diagnosing the time-varying value of forecasts in multiobjective reservoir control. *Journal of Water Resources Planning and Management*, *147*(7), 04021031.

EDC. (2016). *Annual Report 2016* (Tech. Rep.). Electricité du Cambodge (EDC).

Galelli, S., Dang, T. D., Ng, J. Y., Chowdhury, A. K., & Arias, M. E. (2022). Opportunities to curb hydrological alterations via dam re-operation in the mekong. *Nature Sustainability*, *5*(12), 1058–1069.

Galelli, S., Goedbloed, A., Schwanenberg, D., & van Overloop, P. (2014). Optimal real-time operation of multipurpose urban reservoirs: Case study in Singapore. *Journal of Water Resources Planning and Management*, *140*(4), 511–523.

Galelli, S., Humphrey, G. B., Maier, H. R., Castelletti, A., Dandy, G. C., & Gibbs, M. S. (2014). An evaluation framework for input variable selection algorithms for environmental data-driven models. *Environmental Modelling & Software*, *62*, 33–51.

Gebretsadik, Y., Fant, C., Strzepek, K., & Arndt, C. (2016). Optimized reservoir operation model of regional wind and hydro power integration case study: Zambezi basin and South Africa. *Applied Energy*, *161*, 574–582.

Gong, Y., Liu, P., Ming, B., & Li, D. (2021). Identifying the effect of forecast uncertainties on hybrid power system operation: A case study of Longyangxia hydro–photovoltaic plant in China. *Renewable Energy*, *178*, 1303–1321.

Grantz, K., Rajagopalan, B., Clark, M., & Zagona, E. (2005). A technique for incorporating large-scale climate information in basin-scale ensemble streamflow forecasts. *Water Resources Research*, *41*(10).

Guo, Y., Xu, Y., Xie, J., Chen, H., Si, Y., & Liu, J. (2021). A weights combined model for middle and long-term streamflow forecasts and its value to hydropower maximization. *Journal of Hydrology*, *602*, 126794.

Harrigan, S., Zsoter, E., Barnard, C., Wetterhall, F., Ferrario, I., Mazzetti, C., ... Prudhomme, C. (2021). *River discharge and related historical data from the Global Flood Awareness System, v3.1, Copernicus Climate Change Service (C3S) Climate Data Store (CDS).* Retrieved from `https://doi.org/10.24381/cds.a4fdd6b9`

Hong, T., & Fan, S. (2016). Probabilistic electric load forecasting: A tutorial review. *International Journal of Forecasting*, *32*(3), 914–938.

Huang, Z., & Zhao, T. (2022). Predictive performance of ensemble hydroclimatic forecasts: Verification metrics, diagnostic plots and forecast attributes. *Wiley Interdisciplinary Reviews: Water*, *9*(2), e1580.

Ibanez, E., Magee, T., Clement, M., Brinkman, G., Milligan, M., & Zagona, E. (2014). Enhancing hydropower modeling in variable generation integration studies. *Energy*, *74*, 518–528.

JICA. (2014). *Preparatory survey for Phnom Penh city transmission and distribution system expansion project phase II in the Kingdom of Cambodia* (Tech. Rep.). Japan International Cooperation Agency (JICA).

Kern, J. D., Su, Y., & Hill, J. (2020). A retrospective study of the 2012–2016 California drought and its impacts on the power sector. *Environmental Research Letters*, *15*(9).

Koh, R. (2023). PowNetRes_FC: Initial release (v1.0). Zenodo. [Dataset and Software]. Retrieved from `https://doi.org/10.5281/zenodo.8163034`

Koh, R., Kern, J., & Galelli, S. (2022). Hard-coupling water and power system models increases the complementarity of renewable energy sources. *Applied Energy*, *321*, 119386.

Lee, D., Ng, J., Galelli, S., & Block, P. (2022). Unfolding the relationship between seasonal forecast skill and value in hydropower production: A global analysis. *Hydrology and Earth System Sciences*, *26*(9), 2431–2448.

Li, W., Sankarasubramanian, A., Ranjithan, R., & Brill, E. (2014). Improved regional water management utilizing climate forecasts: An interbasin transfer model with a risk management framework. *Water Resources Research*, *50*(8), 6810–6827.

Lima, C., & Lall, U. (2010). Climate informed monthly streamflow forecasts for the Brazilian hydropower network using a periodic ridge regression model. *Journal of hydrology*, *380*(3–4), 438–449.

Liu, P., Guo, S., Xu, X., & Chen, J. (2011). Derivation of aggregation-based joint operating rule curves for cascade hydropower reservoirs. *Water Resources Management*, *25*, 3177–3200.

MacLeod, D., Easton-Calabria, E., de Perez, E., & Jaime, C. (2021). Verification of forecasts for extreme rainfall, tropical cyclones, flood and storm surge over Myanmar and the Philippines. *Weather and climate extremes*, *33*, 100325.

McInerney, D., Thyer, M., Kavetski, D., Laugesen, R., Tuteja, N., & Kuczera, G. (2020). Multi-temporal hydrological residual error modeling for seamless subseasonal streamflow forecasting. *Water Resources Research*, *56*(11), e2019WR026979.

Nash, J. E., & Sutcliffe, J. V. (1970). River flow forecasting through conceptual models part I—A discussion of principles. *Journal of hydrology*, *10*(3), 282–290.

Nayak, M., Herman, J., & Steinschneider, S. (2018). Balancing flood risk and water supply

in California: Policy search integrating short-term forecast ensembles with conjunctive use. *Water Resources Research*, *54*(10), 7557–7576.
Ogliari, E., Guilizzoni, M., Giglio, A., & Pretto, S. (2021). *Renewable Energy*, *178*, 1466–1474.
Oliveira, R., & Loucks, D. (1997). Operating rules for multireservoir systems. *Water Resources Research*, *33*(4), 839–852.
Pastor, A. V., Ludwig, F., Biemans, H., Hoff, H., & Kabat, P. (2014). Accounting for environmental flow requirements in global water assessments. *Hydrology and Earth System Sciences*, *18*(12), 5041–5059.
Pianosi, F., & Soncini-Sessa, R. (2009). Real-time management of a multipurpose water reservoir with a heteroscedastic inflow model. *Water Resources Research*, *45*(10).
Quedi, E., & Fan, F. (2020). Sub seasonal streamflow forecast assessment at large-scale basins. *Journal of Hydrology*, *584*, 124635.
Slater, L. J., Villarini, G., Bradley, & A., A. (2016). Evaluation of the skill of north-American multi-model ensemble (NMME) global climate models in predicting average and extreme precipitation and temperature over the continental USA. *Climate Dynamics*, *53*, 7381-–7396.
Soncini-Sessa, R., Weber, E., & Castelletti, A. (2007). *Integrated and participatory water resources management-theory.* Amsterdam, The Netherlands: Elsevier.
Troin, M., Arsenault, R., Wood, A. W., Brissette, F., & Martel, J.-L. (2021). *Generating ensemble streamflow forecasts: A review of methods and approaches over the past 40 years* (Vol. 56) (No. 7). Wiley Online Library.
Turner, S., Bennett, J. C., Robertson, D. E., & Galelli, S. (2017). Complex relationship between seasonal streamflow forecast skill and value in reservoir operations. *Hydrology and Earth System Sciences*, *21*(9), 4841–4859.
Turner, S., Xu, W., & Voisin, N. (2020). Inferred inflow forecast horizons guiding reservoir release decisions across the United States. *Hydrology and Earth System Sciences*, *24*(3), 1275-1291.
Veloza, O., & Santamaria, F. (2016). Analysis of major blackouts from 2003 to 2015: Classification of incidents and review of main causes. *The Electricity Journal*, *29*(7), 42–49.
Voisin, N., Dyreson, A., Fu, T., O'Connell, M., Turner, S. W., Zhou, T., & Macknick, J. (2020). Impact of climate change on water availability and its propagation through the Western US power grid. *Applied Energy*, *276*, 115467.
Voisin, N., Hamlet, A. F., Graham, L. P., Pierce, D. W., Barnett, T. P., & Lettenmaier, D. P. (2006). The role of climate forecasts in Western U.S. power planning. *Journal of Applied Meteorology and Climatology*, *45*(5), 653–673.
Wang, F., Wang, L., Zhou, H., Saavedra Valeriano, O., Koike, T., & Li, W. (2012). Ensemble hydrological prediction-based real-time optimization of a multiobjective reservoir during flood season in a semiarid basin with global numerical weather predictions. *Water Resources Research*, *48*(7).
Yassin, F., Razavi, S., Elshamy, M., Davison, B., Sapriza-Azuri, G., & Wheater, H. (2019). Representation and improved parameterization of reservoir operation in hydrological and land-surface models. *Hydrol. Earth Syst. Sci.*, *23*(9), 3735–3764.
Yossef, N., Winsemius, H., Weerts, A., van Beek, R., & Bierkens, M. (2013). Skill of a global seasonal streamflow forecasting system, relative roles of initial conditions and meteorological forcing. *Water Resources Research*, *49*(8), 4687–4699.
Zhao, T., Yang, D., Cai, X., Zhao, J., & Wang, H. (2012). Identifying effective forecast horizon for real-time reservoir operation under a limited inflow forecast. *Water Resources Research*, *48*(1).
Zimmerman, B., Vimont, D., & Block, P. (2016). Utilizing the state of ENSO as a means for season-ahead predictor selection. *Water Resources Research*, *52*(5), 3761–3774.
Zsoter, E., Harrigan, S., Barnard, C., Blick, M., Ferrario, I., Wetterhall, F., & Prudhomme, C. (2020). *Reforecasts of river discharge and related data by the Global Flood Awareness System, v2.2, Copernicus Climate Change Service (C3S) Climate Data Store*

(CDS). Retrieved from https://doi.org/10.24381/cds.2d78664e

Supporting Information for: Evaluating Streamflow Forecasts in Hydro-Dominated Power Systems–When and Why They Matter

Rachel Koh [1], Stefano Galelli [1,2]

[1]Pillar of Engineering Systems and Design, Singapore University of Technology and Design, Singapore

[2]School of Civil and Environemntal Engineering, Cornell University, Ithaca, NY

Contents of this file

Text S1. The rule curve of each reservoir is defined as a piece-wise linear function based on four parameters: the minimum and maximum water levels that a reservoir should reach within a year (H_1 and H_2) and the time at which the two levels should be reached (T_1 and T_2). As illustrated in Figure S1, there are three water levels that divide the storage into four zones. These levels are the dead water (or minimum elevation) level, the target water level, and the full (or maximum elevation) level. H_1 and H_2 cannot exceed the dead and critical water levels (H_{min} and H_{max}), respectively. The release dynamics when the reservoir water levels are in Zones 1, 2, and 3 are defined by Eq. 1.

$$R_d = \begin{cases} 0 & \text{if } S_d \leq H_{min} \text{ (Zone 1)} \\ 0 & \text{if } \ H_{min} \leq S_d \leq S_{ts,d_{modT}} \\ & \ \text{and } \ S_{d-1} + Q_d \leq S_{ts,d_{modT}} \\ & \ \text{(Zone 2, case 1)} \\ S_{ts,t_{modT}} - (S_{d-1} + Q_d) & \text{if } \ H_min \leq S_d \leq S_{ts,d_{modT}} \\ & \ \text{and } \ S_{d-1} + Q_d > S_{ts,d_{modT}} \\ & \ \text{(Zone 2, case 2)} \\ (S_{d-1} + Q_d) - S_{ts,d_{modT}} & \text{if } \ S_{ts,d_{modT}} \leq S_d \leq S_{cap} \\ & \ \text{and } \ S_{d-1} + Q_d - R_{max} \leq S_{ts,d_{modT}} \\ & \ \text{(Zone 3, case 1)} \\ R_{max} & \text{if } \ S_{ts,d_{modT}} \leq S_d \leq S_{cap} \\ & \ \text{and } \ S_{d-1} + Q_d - R_{max} > S_{ts,d_{modT}} \\ & \ \text{(Zone 3, case 2)} \end{cases} \tag{1}$$

where $S_{ts,d_{modT}}$ is the target storage at time t_{modT} (in our study, we use a period T of 365 days).

If the water level falls below the dead water level (Zone 1), the turbines are not operated. If the level is between the dead water and target level (Zone 2), the model first uses the information on the incoming daily inflow to solve a mass balance equation, in which the discharge from the dam is kept at zero. The aim is to understand whether the water level is expected to go beyond the target at the end of the day. If that is the case, the model discharges through the turbines the amount of water needed to keep the level close to the target. Otherwise, the turbines are not activated. In Zone 3 (between the target and full level), the turbines are used at their maximum capacity, until the water reaches the target level. In Zone 4 (i.e., level above the maximum elevation), both turbines and spillways are used.

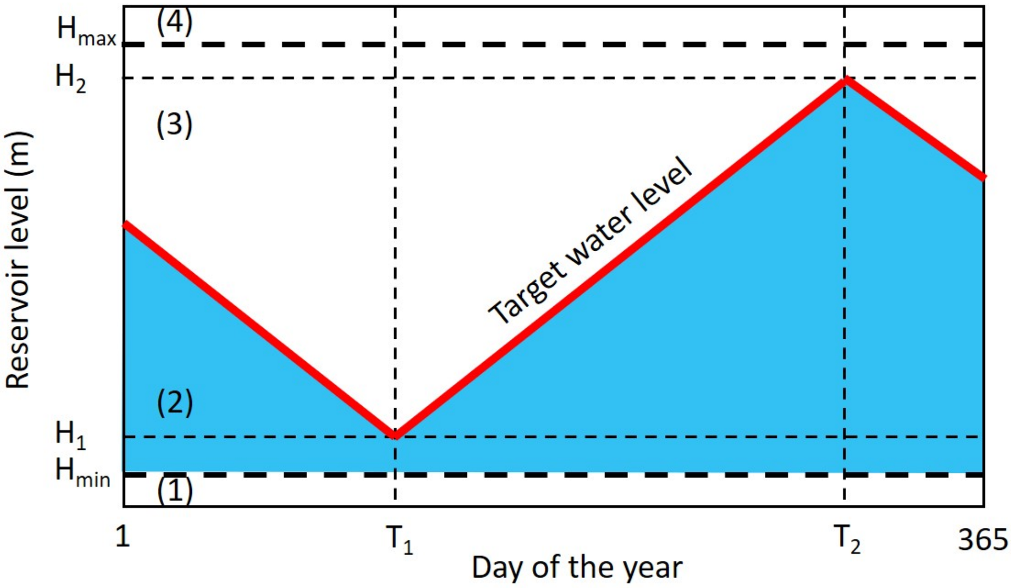

Figure S1. Rule curve.

.

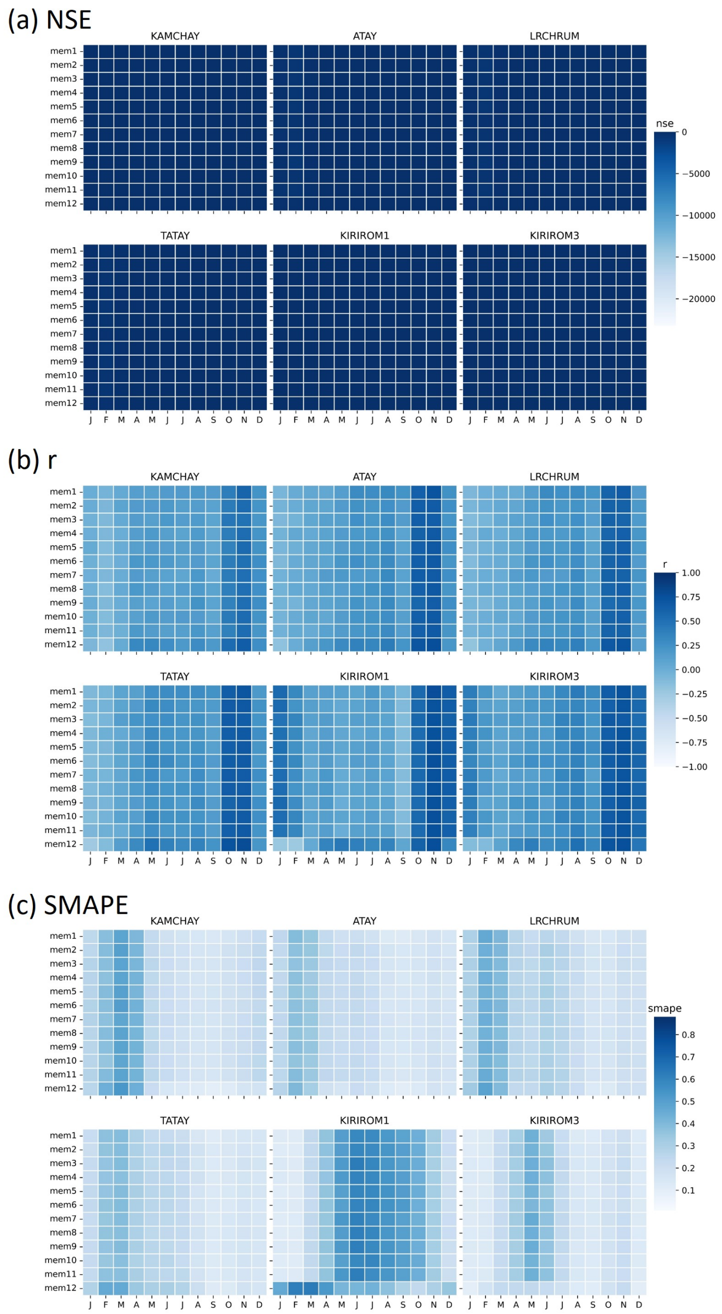

Figure S2. The average streamflow forecast skill of each ensemble member, measured in terms of (a) NSE, (b) r and (c) SMAPE. The six subgrids within each panel represent the six reservoirs in our case study. The range of the forecast metrics can be seen in the colorbar on the right of each panel. As seen in panel (a), NSE can go as low as -20000, amplifying the errors when we do a weighted aggregation. In panel (b), r is bounded by -1 and 1, subjecting them to the possibility of being cancelled out during aggregation. In panel (c), SMAPE ranges between 0 and 1, avoiding the two problems highlighted above.

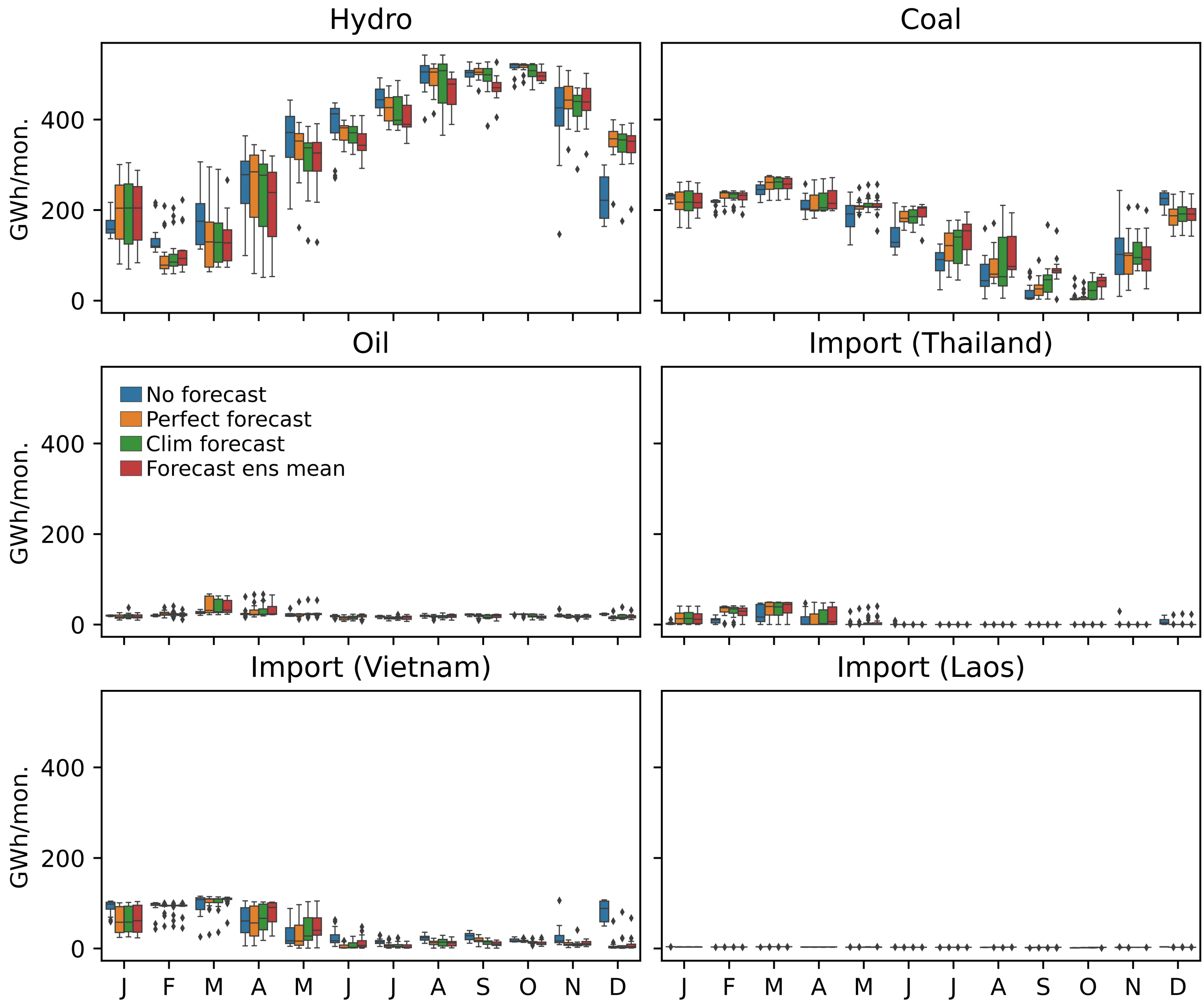

Figure S3. Monthly variability in Cambodia's generation mix under different forecast scenarios. All variables are spatially aggregated for the entire system. Within each panel, the results from three forecast scenarios (perfect, climatology forecast, and the forecast ensemble mean) are compared to the benchmark (no forecast).

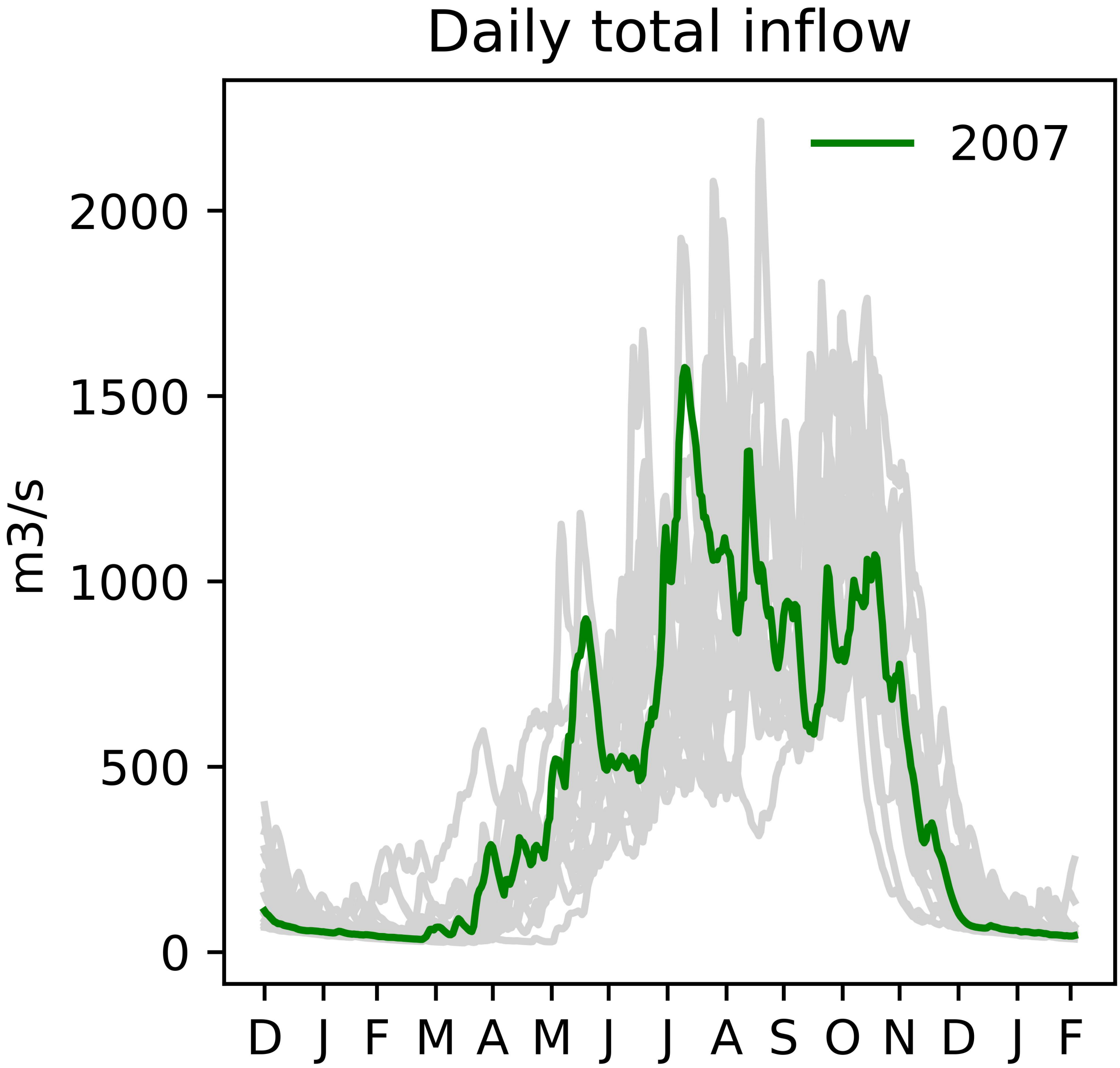

Figure S4. Daily reservoir inflow. Each gray line represents one year between 2000 and 2018. The profile for 2007 is highlighted in green.

Table S1. The generation mix obtained using streamflow forecasts under different scenarios (perfect, climatology and no forecast) under different forecast horizons, simulated over 19 years (2000-2018).

Forecast horizon	Generation mix over 19 years (% of total generation) hydro	coal	imp (Laos)	imp (Thai)	imp (Viet)	oil	slack	Metrics Cost	CO_2	% HP dispatched
Perfect forecast										
7	61.3	25.4	0.48	1.58	7.18	4.03	0.03	3078.5	37.48	82.0
14	62.1	25.0	0.48	1.54	6.82	4.00	0.04	3014.4	36.97	81.9
21	62.0	25.8	0.48	1.46	6.33	3.84	0.03	3016.3	37.90	83.3
30	61.6	27.0	0.49	1.40	6.24	3.76	0.03	3085.9	39.36	84.4
46	57.7	30.4	0.50	1.34	6.44	3.65	0.02	3345.8	43.74	86.9
Climatology forecast										
14	61.4	25.4	0.49	1.59	7.02	4.01	0.03	3068.1	37.53	82.4
30	59.7	28.0	0.49	1.47	6.53	3.75	0.04	3192.3	40.70	84.9
No forecast										
-	60.7	25.5	0.49	0.82	8.71	3.77	0.00	3129.8	37.39	81.7